Document downloaded from:

http://hdl.handle.net/10251/189473

This paper must be cited as:

Hernández-García, J.; Sun, R.; Serrano-Mislata, A.; Inoue, K.; Vargas-Chávez, C.; Esteve-Bruna, D.; Arbona, V.... (2021). Coordination between growth and stress responses by DELLA in the liverwort Marchantia polymorpha. Current Biology. 31(16):1-33. https://doi.org/10.1016/j.cub.2021.06.010

The final publication is available at

https://doi.org/10.1016/j.cub.2021.06.010

Copyright Elsevier

Additional Information

Manuscript Click here to view linked References

Coordination between growth and stress responses by DELLA in the liverwort *Marchantia polymorpha*

Jorge Hernández-García,[1,5] Rui Sun,[2,5] Antonio Serrano-Mislata,[1] Keisuke Inoue,[2] Carlos Vargas-Chávez,[3] David Esteve-Bruna,[1] Vicent Arbona,[4] Shohei Yamaoka,[2] Ryuichi Nishihama,[2,6] Takayuki Kohchi,[2,*] and Miguel A. Blázquez[1,*]

[1] Instituto de Biología Molecular y Celular de Plantas (CSIC-Universitat Politècnica de València), C/Ingeniero Fausto Elio s/n, 46022 Valencia, Spain

[2] Graduate School of Biostudies, Kyoto University, Kyoto 606-8502, Japan

[3] Institute of Evolutionary Biology (CSIC-Universitat Pompeu Fabra), Passeig de la Barceloneta 37-49, Barcelona, Spain.

[4] Departament de Ciències Agràries i del Medi Natural, Universitat Jaume I, Avda. Sos Baynat s/n, 12071 Castellón de la Plana, Spain

[5] Co-first authors

[6] Present address: Department of Applied Biological Science, Faculty of Science and Technology, Tokyo University of Science, 2641 Yamazaki, Noda, Chiba 278-8510, Japan

[*] Correspondence: mblazquez@ibmcp.upv.es, tkohchi@lif.kyoto-u.ac.jp

Lead contact: Miguel A. Blázquez

Summary (250 words, w. references)

Plant survival depends on the optimal use of resources under variable environmental conditions. Among the mechanisms that mediate the balance between growth, differentiation, and stress responses, the regulation of transcriptional activity by DELLA proteins stands out. In angiosperms, DELLA accumulation promotes defense against biotic and abiotic stress and represses cell division and expansion, while the loss of DELLA function is associated with increased plant size and sensitivity towards stress[1]. Given that DELLA protein stability is dependent on gibberellin (GA) levels[2], and GA metabolism is influenced by the environment[3], this pathway is proposed to relay environmental information to the transcriptional programs that regulate growth and stress responses in angiosperms[4,5]. However, *DELLA* genes are also found in bryophytes, whereas canonical GA receptors have been identified only in vascular plants[6–10]. Thus, it is not clear whether these regulatory functions of DELLA predated or emerged with typical GA signaling. Here we show that, as in vascular plants, the only DELLA in the liverwort *Marchantia polymorpha* also participates in the regulation of growth and key developmental processes, and promotes oxidative stress tolerance. Moreover, part of these effects is likely caused by the conserved physical interaction with the MpPIF transcription factor. Therefore, we suggest that the role in the coordination of growth and stress responses was already encoded in the DELLA protein of the common ancestor of land plants, and the importance of this function is underscored by its conservation over the past 450 M years.

Gibberellin, *Marchantia polymorpha*, plant growth, oxidative stress, plant hormone, plant evolution

Results and Discussion

MpDELLA accumulation affects cell division

The genome of *M. polymorpha* encodes a single Mp*DELLA* gene (Mp5g20660)[7,11]. Attempts to generate Mp*della* loss-of-function mutants with several sgRNAs yielded only mutations that did not significantly alter the protein sequence (*i.e.*, the locus was editable, but hypomorphic alleles were not

recovered) (Figure S1A). Whether this is due to lethality or impaired recovery of mutant transgenic plants is presently unknown. Lethality caused by loss of DELLA function has not been previously reported; however, DELLA hypomorphic mutants show defects in gamete formation[12]. Given that the life cycle of *M. polymorpha* is dominated by the haploid phase, we cannot rule out that MpDELLA is also essential for gametophyte survival. Thus, to investigate its biological function, we generated transgenic plants overexpressing Mp*DELLA* either under the control of the CaMV *35S* promoter, or the *M. polymorpha ELONGATION FACTOR1α* (Mp*EF1α*) promoter. In all cases, Mp*DELLA* constitutive overexpression lines displayed smaller thallus sizes than the wild type, which was already evident in two-week-old plants (Figures 1A, 1C, and S1B). To test MpDELLA function within its native expression range, plants were also transformed with additional copies of the gene including its own promoter, coding sequence and a translationally fused β-glucuronidase reporter (*g*Mp*DELLA-GUS*). These lines were moderately high in MpDELLA expression (Figure S1B) but also showed significantly smaller thallus (Figures 1A and 1C). Introducing additional copies, native-promoter driven translational fusion with the β-glucuronidase (GUS) reporter (*g*Mp*DELLA-GUS*) had a moderate, but similar effect (Figures 1A, 1C, and S1B). As members of the GRAS family of transcriptional regulators, DELLA proteins have been shown to function in the nuclei of angiosperms[13,14]. Nuclear localization was also observed for MpDELLA-Cit fusion proteins (Figure S1D). Following such observation, we constructed the inducible Mp*DELLA-GR* lines, which constitutively expressed Mp*DELLA* fused with the rat glucocorticoid receptor. Dexamethasone (DEX)-induced growth impairment was observed in a dose-dependent manner (Figure S1E and S1F). These results support the hypothesis that DELLA accumulation inhibits vegetative growth in *M. polymorpha* and is similar to size alterations observed in several flowering plant species[15–18].

In Arabidopsis, one of the mechanisms proposed for controlling plant size is the DELLA-dependent reduction of cell proliferation rate[19–21]. To investigate if cell division is affected in Mp*DELLA* overexpression lines, we labelled S-phase cells with 5-ethynyl-2′-deoxyuridine (EdU) and observed the nuclear signals around the apical region. All overexpression lines showed significant reduction in the total number of EdU-positive nuclei, which were distributed in a smaller area

compared with wild-type plants (Figures 1B, 1D-E, and S1G-I). For further confirmation of the cell-cycle regulation by Mp*DELLA*, we introduced a G2-M phase reporter (*pro*Mp*CYCB;1:Dbox-GUS*) into the Mp*DELLA-GR* background. After a two-day treatment with 1 μM DEX, the spatial range of GUS signals was notably restricted compared to the mock group (Figure 1F), suggesting a reduction in active cell division.

Histochemical analysis of transcriptional and translational GUS reporters showed that MpDELLA is broadly expressed in the thallus, but the natively expressed MpDELLA protein preferentially accumulated in the apical notch region, where cell division actively occurs (Figures 1G and S1J). This result is comparable with the observations in Arabidopsis showing that DELLA proteins are expressed in the shoot and root apical meristems[20,22,23]. Therefore, Mp*DELLA* may also restrict growth by inhibiting cell proliferation in the meristematic regions of *M. polymorpha*.

Cyclin-dependent kinase inhibitors (CKIs) have been shown to participate in the DELLA-mediated decrease of cell proliferation in Arabidopsis[19,20]. The *M. polymorpha* genome contains two CKI genes, Mp*SMR* (Mp1g14080) and Mp*KRP* (Mp3g00300), which belong to the plant-specific SIAMESE (SIM) protein family and the conserved Kip-related proteins (KRP), respectively[11]. To test genetically if MpDELLA acts through MpSMR to control thallus size, we introduced Mp*SMR* loss-of-function mutations into a Mp*DELLA-GR* line using the CRISPR/Cas9 system[24] (Figure S1K) and examined growth in the absence and the presence of DEX. Gemmalings carrying the Mp*smr*^{ge} alleles were moderately larger than the wild type in mock conditions. More importantly, the growth inhibition caused by activation of Mp*DELLA-GR* was attenuated in the Mp*smr*^{ge} mutants (Figure 1G), supporting the functional relevance of cell division in Mp*DELLA*-mediated growth restriction. Mp*smr*^{ge} alleles did not fully abolish the response to DEX induction, indicating that Mp*DELLA* might also suppress cell proliferation through additional pathways.

Taken together, these results suggest that the regulation of plant size through the interference with cell division is a shared DELLA function in land plants.

MpDELLA regulates development through physical interaction with MpPIF

Distribution of the *g*Mp*DELLA-GUS* signal was also detectable inside gemmae cups, preferentially in developing gemmae (Figures 1H and S1J). Interestingly, both constitutive and induced Mp*DELLA* overexpression exhibited a loss of gemma dormancy, revealed by early gemma germination inside the gemma cups (Figures 2A and 2B). This effect on gemma dormancy resembles the capacity to germinate in the dark of Mp*pif*^{ko}, which is a loss-of-function mutant of Mp*PHYTOCHROME INTERACTING FACTOR* (Mp*PIF,* Mp3g17350)[25]. Indeed, we observed a similar loss of dormancy in gemma cups of Mp*pif*^{ko} lines (Figures 2C and S2A). Reciprocally, DEX induction was found to promote gemma germination in darkness in the Mp*DELLA-GR* lines (Figure S2B). In addition, Mp*DELLA* overexpression lines, including *g*Mp*DELLA-GUS*, displayed a significant delay in the induction of sexual reproduction (Figure 2D), which has also been observed in Mp*pif*^{ko} [26]. These similarities indicate a possible functional connection between Mp*DELLA* and Mp*PIF*, which has been previously reported in Arabidopsis for the regulation of apical hook formation and other developmental processes[27–29].

In Arabidopsis, DELLA proteins interact physically with the PIF transcription factors and prevent their binding to downstream targets[28,29]. It is likely that this mechanism is also conserved in *M. polymorpha*, since we observed that MpDELLA interacts physically with MpPIF in a yeast two-hybrid assay and *in vivo* by co-immunoprecipitation and Bimolecular Fluorescence Complementation assays (Figures 2E, 2F and S2C). Further MpPIF deletion analyses suggested that the GRAS domain of the MpDELLA protein specifically interacts with the bHLH domain of MpPIF (Figures S2D and S2E), paralleling results seen in Arabidopsis[28]. The inhibitory effect of the interaction was verified by dual-luciferase transactivation assays in tobacco. In a dose-dependent manner, MpDELLA inhibited the MpPIF-activation of the At*PIL1* promoter (Figure 2G), a known direct target for PIFs in Arabidopsis[30].

To assess the biological relevance of the interaction between MpDELLA and MpPIF, we tested if an increase in the dosage of MpPIF would suppress the phenotypical defects caused by high MpDELLA levels. Indeed, the reduction of gemma dormancy in gemma cups caused by MpDELLA induction was notably attenuated in $_{pro}$*35S*:*Cit*-Mp*PIF* Mp*DELLA-GR* plants (Figures 2H and S1B-C). Similarly, gemma germination in darkness and the delay in gametangiophore

formation of Mp*DELLA-GR* plants were significantly suppressed in the presence of higher Mp*PIF* levels, both in the absence and presence of DEX treatments (Figures 2I and S2F). No rescue of plant growth by elevated Mp*PIF* levels was observed in the double overexpression lines (Figure S2G). Given the normal vegetative growth of Mp*pif*^{ko} [25], the cell-cycle-repressing function of MpDELLA does not appear to be mediated by MpPIF.

These results suggest that DELLA/PIF-mediated modulation of developmental programs could be a conserved mechanism that was already present in the common ancestor of land plants.

MpDELLA promotes flavonoid accumulation and oxidative stress tolerance

To investigate the downstream targets of the MpDELLA-MpPIF module, we analyzed the transcriptomic changes in $_{pro}$*35S:*Mp*DELLA-Cit* lines and the Mp*pif*^{ko} mutant. As MpPIF proteins are stabilized by far-red light[25], Mp*pif*^{ko} plants were evaluated at 0, 1, or 4 hours after far-red light irradiation (see STAR Methods). Mp*DELLA* overexpression caused the upregulation of 1483 genes and the downregulation of 560 genes (Figure 3A and Data S1). The analysis of differential gene expression in the Mp*pif*^{ko} mutant yielded a total of 339 and 333 genes, up- and down-regulated at least at one time point, respectively (Data S1). As expected, the most abundant set of Mp*PIF*-regulated genes was obtained after the 4-hour far-red treatment (Figure S3A), so we used this set for further analyses. More than half of the upregulated genes in Mp*pif*^{ko} were also upregulated in $_{pro}$*35S*:Mp*DELLA*, and there was a statistically significant overlap also among genes downregulated in both genotypes (Figure 3A), indicating a strong correlation between Mp*DELLA* overexpression and loss of Mp*PIF* functions. As a confirmation, three differentially expressed genes were tested by qPCR, and they all showed expression changes consistent with the RNA-seq (Figure S3B).

Gene ontology enrichment analysis highlighted the regulation of stress response and secondary metabolism processes in both $_{pro}$*35S:*Mp*DELLA-Cit* and Mp*pif*^{ko} upregulated datasets, especially with the enrichment of terms involving phenylpropanoid and flavonoid biosynthesis (Figure 3B and Data S1). In particular, many genes encoding PHENYLALANINE AMMONIA LYASE (PAL),

CINNAMATE 4-HYDROXYLASE (C4H) or CHALCONE SYNTHASE (CHS) were indeed upregulated, as also confirmed by qPCR (Figures 3C and 3D). In the case of Mp*pif*^{ko}, the observed net upregulation of flavonoid biosynthesis genes was mainly due to far-red-induced downregulation in the wild type (Figure S3C), suggesting a suppressive role for MpPIF.

Staining with diphenylboric acid 2-aminoethyl ester confirmed the increased accumulation of flavonoid compounds caused by Mp*DELLA* overexpression or Mp*PIF* loss-of-function (Figures 4A and S4A). Furthermore, the Mp*DELLA*-induced increase of flavonoid signals was less evident when Mp*PIF* is also overexpressed in Mp*DELLA-GR* (Figure S4B). Quantitative analysis of flavonoids showed increases in luteolin 7′-O-glucuronide, and 4′,7-dihydroxyflavan-3-ol content in Mp*DELLA* overexpression lines and Mp*pif*^{ko} *plants* (Figure S4C and Table S1). Similar to other plants, increased flavonoid biosynthesis is a protective response against UV-B-induced oxidative stress in *M. polymorpha*[31]. The ability to enhance the production of these antioxidant compounds suggests a general function for MpDELLA in this stress response, which might be fulfilled in coordination with its inhibition of MpPIF.

To test if MpDELLA levels influence the response to oxidative stress, we examined the tolerance of plants overexpressing Mp*DELLA* to methyl viologen (MV), an inducer of oxidative stress[32]. Six-day-old gemmalings were transferred to plates containing 100 µM MV for 10 days, after which they were allowed to recover for at least one week. All Mp*DELLA* overexpressing plants, including those with the native Mp*DELLA* promoter, showed a significantly higher survival rates compared to wild-type plants (Figure 4B). These results suggest that the increased production of flavonoids caused by higher Mp*DELLA* levels could be responsible for the protection against oxidative stress. This hypothesis is further supported by the observation that Mp*pif*^{ko} mutants also displayed enhanced resistance to MV (Figure 4B), and that the Mp*DELLA*-dependent tolerance was attenuated by Mp*PIF* overexpression (Figure S4D).

In Arabidopsis, the role of DELLAs in the coordination between growth and stress responses is visualized by GA reduction and accumulation of DELLA in response to certain types of stress, coupled to increased tolerance and a variable degree of growth impairment[33]. Although *M. polymorpha* does not possess a GID1-like GA receptor that might modulate MpDELLA protein stability, we found

that exposure of 10-day-old gemmalings to MV provoked an increase in Mp*DELLA* gene expression (Figure 4C and 4D). Such MpDELLA accumulation was concomitant with marked growth arrest and reduced cell division (Figures 4E and S4E). Interestingly, Mp*pif*^{ko} mutants were as large as wild-type plants both in the absence and in the presence of MV (Figure 4E), confirming that the control of *M. polymorpha* thallus size is largely independent of Mp*PIF*.

In summary, we have shown that MpDELLA can modulate cell division, developmental responses and tolerance to oxidative stress in *M. polymorpha* through molecular mechanisms that are shared with angiosperms (Figure 4F). That our results reflect the function of the endogenous MpDELLA protein is supported by the following observations: (i) mild overexpression from the native promoter caused similar phenotypic effects as constitutive and ectopic overexpression; (ii) local induction of MpDELLA-GR in apical notches (where endogenous MpDELLA accumulates) caused growth impairment (Figure S4F-H); and (iii) the effect of MpDELLA accumulation on growth is dose-dependent. The involvement of MpDELLA in growth control is in contrast with the previous proposal that this function emerged with vascular plants, based on the phenotype of *P. patens della* mutants[9]. However, this might reflect a specific functional loss in mosses, given that PpDELLAa still retains the capacity to impair growth in particular contexts, as through heterologous expression in Arabidopsis[9]. Thus, the functional conservation between angiosperm and bryophyte DELLAs implies that the role in the optimization of growth and the responses to disadvantageous environments was already encoded in the ancestral land plant DELLA protein, and the canonical GA signaling might have simply hijacked these functions when the pathway emerged in vascular plants.

Acknowledgements

We thank Eri Nakamura for the pENTR1A-$_{pro}$MpCYCB;1-Dbox plasmid; Shuji Shigenobu and Katsushi Yamaguchi in National Institute for Basic Biology for the help in RNA-seq of Mp*pif*^{ko}; Roberto Solano, Maite Sanmartín and all members of the Plant Plasticity Lab for discussions and insightful comments on the manuscript; and Lynne Yenush for language editing. Work in the authors laboratories has been funded by the Spanish Agencia Estatal de Investigación and FEDER (grants BFU2016-80621-P and PID2019-110717GB to M.A.B) and

JSPS/MEXT KAKENHI (JP17H07424 and JP19H05675 to T.K.; 20H04884 to R.N.). J.H.-G. and A.S.-M. were supported by a predoctoral fellowship from the Spanish Ministry of Education, Culture and Sport (FPU15/01756), and an MSCA Individual Fellowship (H2020-MSCA-IF-2016-746396), respectively. R.S. was supported by the Japanese Government (MEXT) Scholarship Program.

Author Contributions

Conceptualization: M.A.B. and T.K.; Methodology: J.H.-G. and R.S.; Investigation: J.H.-G., R.S., A.S.-M., C.V.-C., D.E.-B., K.I. and V.A.; Writing - Original Draft: J.H.-G., R.S. and M.A.B.; Writing - Review & Editing: J.H.-G., R.S., M.A.B., T.K., S.Y., and R.N.; Visualization: J.H.-G. and R.S.; Funding Acquisition: M.A.B., T.K. and R.N.; Supervision: M.A.B. and T.K.

Declaration of Interests

The authors declare no competing interests.

Figure legends

Figure 1. Mp*DELLA* overexpression inhibits plant growth via cell division.

(A) Morphology of 14-day-old gemmalings in Mp*DELLA* overexpression lines. Scale bar, 5 mm.

(B) Apical notches of 7-day-old gemmalings labelled with EdU (yellow signals). Plant boundaries are marked with white lines, and blue color indicates the area occupied by dividing cells (See STAR methods for definition). Scale bar, 500 μm.

(C) Measurement of plant sizes in 14-day-old gemmalings. n=26 for $_{pro}$*35S:*Mp*DELLA-Cit*; n=27 for others.

(D and E) Number of EdU-labelled nuclei (D) and area of actively dividing regions (E) in the apical notches of 7-day-old gemmalings. n=10 for $_{pro}$Mp*EF:*Mp*DELLA* #5; n=12 for others.

(F) Images of 9-day-old Mp*DELLA-GR* Mp*CYCB;1-GUS* plants stained for GUS activity after mock or 1 μM DEX treatment for 3 days. Scale bar, 1 mm.

(G) A representative image of 21-day-old g*MpDELLA-GUS* plant stained for GUS activity. Scale bar, 500 μm.

(H) Plant sizes of 7-day-old Mps*mr*^{ge} Mp*DELLA-GR* gemmalings after mock or 1 μM DEX treatment for 5 days. Ratio of plant sizes (±propagated SE) for each pair is shown in grey. n=15.

All plants were grown under continuous white light except long-day conditions in H. In C, D, E, H, dots represent individual plants, and the horizontal lines represent mean values. Statistical groups are determined by Tukey's Post-Hoc test ($p<0.05$) following one-way ANOVA.

See also Figure S1.

Figure 2. Functional interaction between MpDELLA and MpPIF.

(A) Gemma dormancy in 28-day-old plants of Mp*DELLA* overexpression lines. Dashed circles indicate non-dormant gemma cups. Scale bar, 5 mm.

(B and C) Proportion of dormant gemma cups in 28-day-old MpDELLA overexpression lines (B) or Mp*pif*^{ko} mutants (C). n=12.

(D) Progress of gametangiophore formation in Mp*pif*^{ko} mutants and Mp*DELLA* overexpression lines. n=9.

(E) Physical interaction between MpDELLA and MpPIF shown by yeast two-hybrid assay. BD and AD denote fusions to the GAL4 DNA binding domain or the activation domain, respectively.

(F) Physical interaction between YFP-MpDELLA and HA-MpPIF shown by co-immunoprecipitation after agroinfiltration in *N. benthamiana* leaves.

(G) Transient expression assay of the At*PIL1:LUC* reporter in *N. benthamiana* leaves after agroinfiltration with different levels of Mp*PIF* and Mp*DELLA* (shown below the graph as infiltrated OD_{600}). n=9 in total.

(H) Quantification of gemma cup dormancy in 30-day-old $_{pro}$*35S:*Mp*PIF-Cit* Mp*DELLA-GR* plants, after treatment with mock or 1 µM DEX for 20 days.

Progress of gametangiophore formation in $_{pro}$*35S:*Mp*PIF-Cit* Mp*DELLA-GR* plants, inducted with far-red light and treated with mock or 1 nM DEX. n=10.

In A, B and C, plants were grown on ½ Gamborg's B5 plates with 1% sucrose under cW. In B, C, and H, dots represent individual plants. In G dots represent biological replicates from three independently performed experiments. All horizontal lines represent total mean values. Statistical groups are determined by Tukey's Post-Hoc test ($p<0.05$) following ANOVA analysis. In D and I, error bars represent standard deviation.

See also Figure S2.

Figure 3. Genome-wide co-regulation of gene expression by MpPIF and MpDELLA.

(A) Venn diagram showing genes differentially expressed in $_{pro}$*35S*:Mp*DELLA-Cit* and in the Mp*pif*^{ko} mutant (after 4 hours of far-red light irradiation). P-values were calculated by Fisher's exact tests.

(B) Two-dimensional t-SNE plot visualizing GO categories over-represented in the sets of genes differentially expressed in $_{pro}$*35S*:Mp*DELLA-Cit* and in Mp*pif*^{ko}.

(C) Heatmap showing gene expression changes of the flavonoid biosynthesis pathway. Asterisks indicate genes considered as significantly changed ($|log2FC|>1$; adjusted $p<0.01$). Black dots in the bottom row indicate genes significantly changed in response to FR irradiation at any time point in either WT or Mp*pif*^{ko}.

(D) Expression level of selected flavonoid biosynthesis genes determined by

RT-qPCR. Error bars represent standard deviation. n=3. *, p<0.05; **, p<0.01 by Student's t-test.

See also Figure S3 and Data S1

Figure 4. Involvement of Mp*DELLA* in the response to oxidative stress.

(A) Images of 14-day-old gemmalings, stained with diphenylboric acid 2-aminoethyl ester to show general flavonoid content. Scale bar, 5 mm.

(B) Percentage of surviving apical notches after a 10-day treatment with 100 µM MV in different transgenic lines. Dots represent independent experiments (n=3).

(C) Relative expression level of Mp*DELLA* determined by RT-qPCR in 14-day-old gemmalings grown in mock or 10 µM MV-supplemented media. Error bars represent standard error; n=3.

(D) GUS-stained Mp*DELLA* reporter lines, showing the increased signals in the apical notches of 13-day-old plants after a 6-day treatment with mock or 10 µM MV.

(E) Size of 14-day-old gemmalings grown on mock or 0.5 µM MV-supplemented medium. n=19 (WT Mock), 16 (WT MV), 36 (Mp*pif*^{ko} Mock), 28 (Mp*pif*^{ko} MV), 25 (*g*Mp*PIF*/Mp*pif*^{ko} Mock), 24 (*g*Mp*PIF*/Mp*pif*^{ko} MV).

(F) Model for the regulation of growth, development and stress responses by Mp*DELLA*. Under stress, MpDELLA would accumulate in apical notches protecting them through the MpPIF-dependent production of antioxidant compounds, and suppressing growth by inhibiting cell divisions. The interaction with MpPIF also causes alterations in developmental processes, such as gemma dormancy or gametangiophore formation.

All plants were grown under long-day conditions. In B, E, dots represent biological replicates, and the horizontal lines represent mean values. Statistical groups were determined by Tukey's Post-Hoc test (p<0.05) following ANOVA analysis.

See also Figure S4 and Table S1

STAR Methods

RESOURCE AVAILABILITY

Lead Contact

Further information and requests for resources and reagents should be directed to and will be fulfilled by the Lead Contact, Miguel A. Blázquez (mblazquez@ibmcp.upv.es).

Materials availability

Plasmids and plant materials generated in this research are all available from the Lead Contact upon request. Please note that the distribution of transgenic plants will be governed by material transfer agreements (MTAs) and will be dependent on appropriate import permits acquired by the receiver.

Data and Code Availability

Raw RNA sequencing datasets generated during this study were deposited to the Short Read Archive at the National Center for Biotechnology Information (NCBI) or the Sequence Read Archive at DNA Data Bank of Japan (DDBJ) under Bioprojects PRJNA695248 and PRJDB11176. The modified ITCN plugin for ImageJ is available at https://github.com/PMB-KU/CountNuclei. R scripts used for processing EdU data, Blast2GO annotation and RNA-seq analysis were deposited to https://github.com/dorrenasun/MpDELLA.

EXPERIMENTAL MODEL AND SUBJECT DETAILS

Plant Materials and Growth Conditions

Marchantia polymorpha accession Takaragaike-1 (Tak-1; male)[34] was used in this study as the wild-type (WT). Female lines Mp*pif*^{ko} and *g*Mp*PIF*/Mp*pif*^{ko} were previously described as *pif*^{KO} #1 and $_{pro}$*PIF:PIF*/*pif*^{KO} #1, respectively[25]. *M. polymorpha* plants were cultured on half-strength Gamborg's B5[35] medium with 1% agar at 21-22ºC. Light conditions are specified in each figure; generally, long day (LD) conditions refer to cycles with 16 hours of light (90-100 µmol m^{-2} s^{-1}) and 8 hours of darkness in a Percival growth chamber (E-30B), while continuous white light (cW) was supplemented at the intensity of 50-60 µmol m^{-2} s^{-1} by cold

cathode fluorescent lamp (CCFL; OPT-40C-N-L, Optrom, Japan) in a growth room.

Nicotiana benthamiana wild-type seeds were sown in pots filled with regular soil mixture from a local provider and covered for a week with a plastic humidity dome after watering. Plants grown in a growth room under long day conditions (16 of light [120 μmol m^{-2} s^{-1}] and 8 hours of darkness) at 24ºC (light) and 20ºC (darkness).

METHOD DETAILS

Cloning and plasmid construction for plant transformation

Various Gateway-compatible entry vectors related to Mp*DELLA* were generated. The full length CDS, GRAS domain (amino acids 173 to 560), promoter (4.3kb upstream of ATG), and genomic (promoter and CDS) regions were amplified from genomic DNA by PCR using Phusion High-Fidelity Polymerase (Thermo Fisher Scientific) with attB-containing primers, and introduced into pDONR221 (Thermo Fisher Scientific) vector using Gateway BP Clonase II Enzyme mix (Thermo Fisher Scientific) to generate pENTR221-MpDELLA, -$MpDELLA^{GRAS}$, -$_{pro}$MpDELLA and -gMpDELLA, respectively. The CDS region was also amplified with KOD FX Neo DNA polymerase (Toyobo Life Science) and directionally cloned into pENTR/D-TOPO (Thermo Fisher Scientific) to create pENTR-MpDELLA. For pENTR1A-$_{pro}$MpDELLA-short, a slightly shorter promoter region was amplified with PrimeSTAR GXL DNA Polymerase (TaKaRa Bio) and inserted between the *Sal*I and *Not*I sites of pENTR1A (Thermo Fisher Scientific) with T4 DNA ligase (TaKaRa Bio). pENTR1A-gMpDELLA-short was further created by seamless integration of the CDS fragment with the In-Fusion Cloning kit (TaKaRa Bio). Finally, both constructs were extended at the 5′ end by In-Fusion insertion to create pENTR1A-$_{pro}$MpDELLA and pENTR1A-gMpDELLA, matching with the lengths of pENTR221 counterparts.

To create the vectors for Mp*DELLA* overexpression, pENTR221-MpDELLA and pENTR211-gMpDELLA were recombined with pMpGWB106 and pMpGWB107[36] using Gateway LR Clonase II Enzyme mix (Thermo Fisher Scientific) to generate pMpGWB106-MpDELLA and pMpGWB107-gMpDELLA,

respectively. pENTR-MpDELLA was recombined with pMpGWB310 and pMpGWB313 for the generation of pMpGWB310-MpDELLA and pMpGWB313-MpDELLA, while pENTR1A-$_{pro}$MpDELLA and pENTR1A-gMpDELLA were recombined with pMpGWB304 to generate pMpGWB304-$_{pro}$MpDELLA and pMpGWB304-gMpDELLA. All these binary vectors were introduced into Tak-1 plants.

To monitor the cell division activity, the promoter (3.8 kb upstream of ATG) and coding sequence of the first 116 amino acids (including the destruction box) of Mp*CYCB;1* (Mp5g10030) was amplified with KOD -Plus- Ver.2 (Toyobo Life Science) and ligated into the the *Sal*I and *Eco*RV sites of pENTR1A (Thermo Fisher Scientific) with Ligation high Ver.2 (Toyobo Life Science). The resulting plasmid was recombined with pMpGWB104 and then transformed into the *M. polymorpha* transgenic line Mp*DELLA-GR* #5.

CRISPR/Cas9-based genome editing of Mp*DELLA* and Mp*SMR* (*Mp1g14080*) was performed as previously described[37]. For Mp*DELLA*, various guide RNAs were designed in the coding sequence and the 5′-untranslated region. For Mp*SMR*, the guide RNA was designed upstream of the CDKI domain with Benchling[38]. Double stranded DNA corresponding to the guide RNA protospacers were generated by annealing complementary oligonucleotides and inserted into BsaI-digested pMpGE_En03[37] by ligation using DNA T4 ligase (Promega), and then transferred to the binary vector pMpGE010[37] using Gateway LR Clonase II Enzyme mix (Thermo Fisher Scientific). *M. polymorpha* transformation was carried out in Tak-1 for Mp*DELLA*, or the transgenic line Mp*DELLA-GR* #5 for Mp*SMR*, as described below.

For the construction of Mp*PIF*-Mp*DELLA* double overexpression lines, the Mp*PIF* (*Mp3g17350*) coding region containing the stop codon was amplified from cDNA, cloned into pENTR/D-TOPO (Thermo Fisher Scientific), then recombined with pMpGWB105 using Gateway LR Clonase II Enzyme mix (Thermo Fisher Scientific). The resulting construct was transformed into the *M. polymorpha* transgenic line Mp*DELLA-GR* #5.

All entry plasmids were confirmed by restriction enzyme digestion and Sanger sequencing. Destination vectors were confirmed by restriction enzyme digestion.

Marchantia polymorpha genetic transformation

All the *M. polymorpha* transgenic lines are listed in the Key Resources Table. Transformants were obtained by agrobacterium-mediated transformation from regenerating thalli, using *Agrobacterium tumefaciens* strains GV3101 (pMP90 C58) or GV2260[39–41]. Briefly, gemmae were grown in standard conditions (either cW or LD), during 14 days and cut into four pieces without apical notches, then cultured for 3 days on standard medium with 1% sucrose to induce regeneration. Regenerating fragments were co-cultured with *A. tumefaciens* in liquid medium with 100 mM acetosyringone with agitation. After three days the plants were washed six times with autoclaved water, incubated for 30 min in 1 mg/mL cefotaxime and plated on selective plates containing 0.5 µM chlorsulfuron or 10 mg/l hygromycin (see Key Resources Table) and 100 mg/l cefaxime.

Regenerating transgenic plants (T1) checked by PCR amplification from crude DNA extracts. Gemmae derived from T1 plants (G1) were confirmed and further descendants used for experiments. For CRISPR/Cas9-based genome editing, G1 plants were checked by PCR amplification followed by Sanger sequencing, to assess genome editing events, and confirmed for stable editing in G2 plants derived from gemmae of G1 plants.

Plant growth and EdU staining

For the measurement of plant sizes, images of the whole culturing plates were taken vertically above with a digital camera (Canon EOS Kiss X7i). The thallus projection areas were analyzed with ImageJ 1.52a[42] by thresholding the images with the default algorithm on the blue color channel and batch-measured with the function “Analyze Particles”.

For the detection of S-phase cells, constitutive- and native-promoter MpDELLA overexpression lines were grown from gemmae for seven days under cW. Mp*DELLA-GR* lines were grown from gemmae under cW for five days, then transferred onto the plates containing mock solvent or 1 µM dexamethasone

(DEX) and cultured for two days. All the plants were labeled with 20 μM 5-ethynyl-2′-deoxyuridine (EdU) in liquid half-strength Gamborg's B5 medium under cW for 2 h. Then they were fixed with 3.7% formaldehyde for 1 h, washed for 5 min twice with phosphate buffer saline (PBS), and permeabilized in 0.5% Triton X-100 in PBS for 20 min. After two 5-min washes with 3% bovine serum albumin (BSA) in PBS, samples were incubated with the reaction mixture from Click-iT EdU Imaging Kit with Alexa Fluor 488 (Invitrogen) in the dark for 1 h. After staining, samples were protected from light, washed twice with 3% BSA in PBS and soaked in ClearSee solution[43] for 3-7 days. After that, the samples were mounted to slides with 50% glycerol and observed with Keyence BZ-X700 all-in-one fluorescence microscope. Z-stacks of fluorescence images were taken in 2-μm steps with the YFP filter (Keyence 49003-UF1-BLA, excitation at 490-510 nm, detection range 520-550 nm) and merged together with the BZ-X Analyzer software (1.3.1.1).

Microscopy & histochemical analysis

For GUS activity assay, plants were vacuum-infiltrated with GUS staining solution (50 mM sodium phosphate buffer pH 7.2, 0.5 mM potassium-ferrocyanide, 0.5 mM potassium-ferricyanide, 10 mM EDTA, 0.01% Triton X-100 and 1 mM 5-bromo-4-chloro-3-indolyl-β-D-glucuronic acid) for 15 min, and then incubated at 37 ºC overnight (>16 hours). Samples were de-stained with 70% ethanol and imaged under an Olympus SZX16 stereoscope. To prepare agar sections, stained samples were embedded in 6% agar and sectioned into 100-μm slices with LinearSlicer PRO 7 (DOSAKA EM, Kyoto, Japan), then imaged with Keyence BZ-X700 microscope in the bright-field.

Confocal laser scanning microscopy on *g*Mp*DELLA-Cit* gemma was performed using a Leica TCS SP8 equipped with HyD detectors. A white light laser was used to visualize Citrine (excitation 509 nm). Diphenylborinic acid 2-aminoethyl ester (DPBA) staining was used to visualize flavonoids as previously described[44]. Whole thalli were stained for 15 minutes at 0.25% (w/v) DPBA and 0.1% (v/v) Triton X-100. Epifluorescence microscopy of stained flavonoids in

gemmalings was performed on a Leica DMS1000 dissecting microscope using a GFP filter for detection of DPBA fluorescence.

Scoring of gemma cup dormancy

To score the dormancy of gemma cups, constitutive- and native-promoter Mp*DELLA* overexpression lines, as well as Mp*pif*^{ko} plants were grown from gemmae on half-strength Gamborg's B5 plates with 1% sucrose under cW for 28 days. Mp*DELLA-GR* and $_{pro}$*35S:Cit*-Mp*PIF* Mp*DELLA-GR* lines were grown on half-strength Gamborg's B5 plates without sucrose under cW for 10 days, then transferred onto plates containing mock solvent or 1 μM DEX and cultured for another 20 days before evaluation. Gemma cups with observable gemmae were observed carefully under stereoscopes, marked on photos taken with a digital camera and then counted. If a gemma with rhizoid and/or growth expansion was observed in a certain gemma cup, it is considered as non-dormant. Representative plants were also photographed with Leica M205C stereo microscopes to show the dormancy of gemma cups in different transgenic lines.

Gemma germination assay

Gemma germination assays were carried out following the previous publication[25]. In each experiment, fifty gemmae of each group were planted onto half-strength Gamborg's B5 plates containing 1% sucrose under green light, then treated with far-red light (30 μmol photons m^{-2} s^{-1}) for 15 minutes. For Mp*DELLA-GR* related experiments, 1 μM DEX or the mock solvent was supplemented in the agar plates. After one day of imbibition in the dark, gemmae were irradiated with nothing or a pulse of red light (4500 μmol photons m^{-2}) and then cultured for another six days in the dark. Photos of each gemmae were taken using Leica M205C or Olympus SZX16, then evaluated for germination based on growth expansion and/or the development of rhizoids.

Gametangiophore formation observation

To monitor the progress of gametangiophore formation in transgenic lines shown in Figure 2B, plants were grown from gemmae on half-strength Gamborg's B5 plates with 1% sucrose under continuous white light (~50 µmol photons m^{-2} s^{-1}, in a CCFL growth cabinet from Nippon Medical & Chemical Instruments, LH-80CCFL-6CT) supplemented with far-red light (~20 µmol photons m^{-2} s^{-1} provided by diodes from Valore, Japan: VBL-TFL600-IR730. Referred to as cW+FR.). Individual plants were examined and counted for visible gametangiophores each day under stereoscopes. For the experiment in Figure 2I, gemmae of inducible lines or the wild-type control were grown on half-strength Gamborg's B5 plates with 1% sucrose with no DEX under cW for 10 days, then half pieces of thallus were transferred onto plates containing 1 nM DEX or mock solvent and cultured under cW+FR. Gametangiophore formation progresses were observed for half plants similarly as described above.

Yeast-two hybrid assays

For yeast two-hybrid analyses, Mp*PIF* full length CDS and CDS fragments were amplified from cDNA and introduced into pCR8 using the pCR8/GW/TOPO TA Cloning Kit (Thermo Fisher Scientific) to generate pCR8-MpPIF and -MpPIFdel1-4. Then they were recombined with pGADT7-GW[45] using Gateway LR Clonase II Enzyme mix (Thermo Fisher Scientific) to produce Gal4-activation domain (AD) fusion proteins. To avoid the previously shown N-terminal transactivation of MpDELLA[7], only the GRAS domain (pENTR221-MpDELLA^{GRAS}) was introduced into pGBKT7-GW[45] to fuse with the GAL4 DNA-binding domain. Yeast transformation was performed by lithium acetate/single-stranded carrier DNA/polyethylene glycol method as previously described[46]. Y187 and Y2HGold yeast strains were transformed with pGADT7 and pGBKT7-derived expression vectors and selected with Synthetic Defined (SD) medium lacking leucine (-Leu) or tryptophan (-Trp), respectively. Subsequently, haploid yeasts were mated to obtain diploid cells by selection in SD/-Leu-Trp medium. Protein interactions were assayed by the nutritional requirement on histidine (His). SD/-Leu-Trp plates were used as growth control, and SD/-Leu-Trp-His plates supplemented with 5 mM 3-amino-1,2,4-triazole (3-AT, Sigma-Aldrich) was used for interaction evaluation. Spotting assays were performed using cultures with optical density =

1 ($OD_{600\ nm}$ = 1) as initial concentration in sequential drop dilutions, and plated with a pin multi-blot replicator. Photos of the same-fold dilutions were taken 3 days after plating.

Co-immunoprecipitation (Co-IP) and Bimolecular Fluorescence Complementation (BiFC) assays

Co-IP vectors were obtained by introducing Mp*DELLA* CDS (pENTR221-Mp*DELLA*) into pEarleyGate104 and MpPIF fragments (pCR8-Mp*PIF* and -Mp*PIFdel3*) into pEarleyGate201 [47]. For BiFC, pENTR211-Mp*DELLA* and pCR8-Mp*PIF* were recombined with pMDC43-YFN and pMDC43-YFC[48], respectively. *Agrobacterium tumefaciens* GV3101 containing binary plasmids for Co-IP and BIFC were used to infiltrate 4-week-old *Nicotiana benthamiana*. Briefly, overnight grown exponential cultures of *A. tumefaciens* were collected by centrifugation, resuspended in agroinfiltration solution (10 mM MES, 20 mM MgCl2, 200 µM acetosyringone, pH 5.6), and incubated at room temperature during 4-6 hours. Resuspended cultures were adjusted to $OD_{600\ nm}$ = 0.1 with agroinfiltration solution and mixed in equal volumes when necessary. Agroinfiltration was carried out through abaxial leaf surfaces using 1 ml needle-free syringes.

For Co-IP, leaves were re-infiltrated with a solution of 25 µM MG-132 8 hours before collection 3 days after *A. tumefaciens* infiltration, grinded in liquid nitrogen and homogenized in 1 ml extraction buffer (50 mM Tris–HCl pH 7.5, 150 mM NaCl, 0.1% Triton, 2 mM PMSF, and 1x protease inhibitor cocktail [Roche]). Proteins were quantified using the Bradford assay. 50 µg of total proteins were stored as input. One milligram of total proteins was incubated for 2 h at 4ºC with anti-GFP-coated paramagnetic beads and loaded onto µColumns (Miltenyi). Wash and elution from beads was performed according to manufacturer's instructions. Samples were analyzed by Western-blot after running two 12% SDS-PAGE gels in parallel. One gel was loaded with 25 µg of input, and 10% of eluted proteins; following wet transfer, the PVDF membrane was incubated with an anti-GFP antibody (JL8, 1:5000). The second gel was loaded with 25 µg of input, and 90% of eluted proteins and, after transfer, the membrane incubated with an anti-HA-HRP antibody (3F10, 1:5000). Chemiluminiscence was detected

with SuperSignal West Femto substrates (Thermo-Fisher Scientific) and imaged with a LAS-3000 imager (Fujifilm).

For BiFC, leaves were analyzed with a Zeiss LSM 780 confocal microscope 3 days after infiltration. Reconstituted YFP signal was detected with emission filters set to 503-517 nm. Nuclei presence in abaxial epidermal cells was verified by transmitted light.

Dual luciferase transactivation assay

Mp*DELLA* and Mp*PIF*-expresssing vectors used for Co-IP (pEarleyGate104-MpDELLA and pEarleyGate201-MpPIF) were used as effector plasmids. A previously available construct with the *Arabidopsis thaliana PIL1* promoter controlling the firefly luciferase gene expression, and a constitutively expressed *Renilla* luciferase gene was used as reporter plasmid[30]. The promoter consists of 1.8 kb upstream of the gene ATG codon, including three consecutive G-boxes known to be bound *in vivo* by PIF3. Transient expression in *N. benthamiana* leaves was carried by agroinfiltration as previously reported[49]. The amount of infiltrated bacteria was set by OD_{600} measurement of A. tumefaciens liquid cultures. Combinations of pre-set reporter-carrying bacteria ($OD_{600\ nm}$ = 0.1) and varying amounts of effector-carrying bacteria were mixed and co-infiltrated together. All the mixes were co-infiltrated alongside *p19* vector-carrying bacteria at a $OD_{600\ nm}$ = 0.01. Firefly (*Photinus pyralis*) and control *Renilla* luciferase activities were assayed in extracts from 1-cm in diameter leaf discs, using the Dual-Glo Luciferase Assay System (Promega) and quantified in a GloMax 96 Microplate Luminometer (Promega). Three leaf disc extracts were quantified per sample in each experiment and repeated for three times. Final quantifications represent means of ratios between firefly luciferase and *Renilla* luciferase read-outs in three independent experiments.

RNA isolation, cDNA synthesis, and RT-qPCR analysis

To examine the expression levels of Mp*DELLA* and Mp*PIF* in different transgenic lines, 14-day-old plants grown under cW were homogenized in liquid nitrogen. Total RNA was isolated with TRIzol reagent (Thermo Fisher Scientific) following

the manufacturer's instructions. After checking the concentration and quality of RNA using a NanoDrop 2000 spectrophotometer (Thermo Scientific), up to 3 µg of total RNA was digested with RQ1 RNase-Free DNase (Promega) and reverse-transcribed using ReverTra Ace (Toyobo Life Science) and an oligo $(dT)_{20}$ primer. Resulting cDNA was diluted 10 times in ddH_2O, and 5 µL was used for each 25-µL quantitative real-time PCR (qPCR) with TaKaRa Ex Taq (TaKaRa Bio) and SYBR Green I Nucleic Acid Gel Stain (Lonza). Reactions were performed in a CFX96 real-time PCR detection system (Bio-Rad), with an initial denaturation step of 30 s at 95 ºC and then cycled for 40 times with 5 s at 95 ºC and 30 s at 60 ºC. At the end of amplification, standard melt curve analysis supplemented by the CFX Maestro software was performed to validate amplified targets.

For other qPCR experiments, total RNA was extracted with a RNeasy Plant Mini Kit (Qiagen) according to the manufacturer's instructions. cDNA was prepared from 1 µg of total RNA with PrimeScript 1st Strand cDNA Synthesis Kit (Takara Bio Inc). Resulting cDNA was diluted 1:9 in ddH_2O and 1 µl of the resulting dilution used in the PCR reaction. PCR was performed in a 7500 Fast Real-Time PCR System (Applied Biosystems) with SYBR premix ExTaq (Tli RNaseH Plus) Rox Plus (Takara Bio Inc), using the comparative C_T standard program implemented in the 7500/7500 Fast Software according to manufacturer's instructions, including melt curve analysis to validate amplified targets.

Sample reactions were pipetted in triplicates per biological replicate and gene. All relative expression levels were calculated following Hellemans *et al.*[50], and Mp*EF1α* (Mp*ELONGATION FACTOR 1α, Mp3g23400*) was used as the reference gene[25]. Primers are listed in Table S2.

RNA sequencing

For the Mp*DELLA* overexpression data set, WT and *pro35S:*Mp*DELLA-Cit* plants were grown from gemmae on half-strength Gamborg's B5 plates containing 1% sucrose under LD conditions for 30 days. Then whole plants for two biological replicates were collected for total RNA extraction total RNA with a RNeasy Plant Mini Kit (Qiagen) according to the manufacturer's instructions. The

RNA concentration and integrity [RNA integrity number (RIN)] were measured with an RNA nanochip (Bioanalyzer, Agilent Technologies 2100). Library preparation with TruSeq RNA Sample Prep Kit v.2 (Illumina) and sequencing of 75-nt single-end reads on Illumina NextSeq 550 were carried out at the Genomics Service of the University of Valencia.

For the Mp*pif*^{ko} dataset, Tak-1 and Mp*pif*^{ko} were grown from gemmae on half-strength Gamborg's B5 plates containing 1% sucrose under continuous red-light conditions (50 µmol photons m^{-2} s^{-1}) for 7 days, then irradiated with far-red light (50 µmol photons m^{-2} s^{-1}). Whole plant materials for three biological replicates were collected each at 0, 1, and 4 h after the irradiation. Total RNAs were extracted using RNeasy Plant Mini Kit (Qiagen) and purified with the RNeasy MinElute Cleanup Kit (Qiagen). RNA concentration and qualities were examined by Qubit Assays (Thermo Fisher Scientific) and the Agilent 2100 Bioanalyzer. Libraries were prepared using a TruSeq RNA Sample Prep Kit v.2 (Illumina), quantified by KAPA Library Quantification Kit (Kapa Biosystems), and sequenced of 126-nt single-end reads on Illumina HiSeq 1500 at National Institute for Basic Biology (Okazaki, Japan).

Non-targeted flavonoid-related metabolite profiling

Analysis of secondary metabolites in freeze-dried Marchantia samples was carried out following a non-targeted approach as previously described[51]. Briefly, samples (c.a. 10 mg) were extracted in 80% aqueous MeOH containing biochanin A at 1 mg L^{-1} (Sigma-Aldrich, Madrid, Spain) as internal standard by ultrasonication for 10 min. Crude extracts were centrifuged and clean supernatants recovered and filtered through PTFE 0.2 µm syringe filters directly into dark chromatography vials. Extracts were injected into a UPLC system (10 µL) (Acquity SDS, Waters Corp. Ltd. USA) and separations carried out on a C18 column (Luna Omega Polar, C18, 1.6 µm, 100 × 2.1 mm, Phenomenex, CA, USA) using acetonitrile and ultrapure water, both supplemented with formic acid at a concentration of 0.1% (v/v), as solvents at a flow rate of 0.3 mL min^{-1}. A gradient elution program starting from 5% to 95% acetonitrile in 17 min followed by a 3 min re-equilibration period was employed. Compounds were detected by mass spectrometry using a hybrid quadrupole time-of-flight mass spectrometer (QTOF-

MS, Micromass Ltd., UK) coupled to the UPLC system through an electrospray source. Samples were analyzed in both positive and negative electrospray modes within 50-1000 Da mass range using two simultaneous acquisition modes: 1) low CID energy for profiling purposes and 2) high CID energy for MS/MS of selected compounds, this was achieved by setting an energy ramp from 5-60 eV. During measurements cone and capillary voltages were set at 30 V and 3.5 kV, respectively; source and block temperatures were kept at 120ºC. Desolvation gas (N_2) was kept at 350 ºC at a flow rate of 800 L h^{-1}. Nebulization gas was also N_2 at a flow rate of 60 L h^{-1}. In the collision cell, pure Ar was used as the collision gas. Exact mass measurements were achieved by monitoring the reference compound lockmass leucine-enkephalin ([M+H]+ 556.2771 and [M-H]− 554.2514, respectively); therefore, the resulting mass chromatograms were acquired in centroid mode.

Analysis of survival after oxidative stress

For survival measurement, 10 gemmae per genotype and experiment were grown on top of Whatman filter papers discs (Thermo Fisher) on half-strength Gamborg's B5 1% agar medium for 6 days, and then transferred to half-strength Gamborg's B5 1% agar medium supplemented with 100 µM methyl viologen to produce a severe oxidative stress for 10 days. Gemmallings were transferred back to half-strength Gamborg's B5 1% agar medium for recovery. Survival was counted when independent apical regions resumed growth and represented as the percentage of growth-resuming apical regions of the total number at the beginning of the stress treatment.

In Mp*DELLA-GR* related assays, the same procedure was followed, but mock and 1 µM dexamethasone (DEX) were included for DELLA activity induction during the 10 days of oxidative stress treatment. In addition, DEX or mock (ethanol) were added in water solution 24 hours before stress treatment.

QUANTIFICATION AND STATISTICAL ANALYSIS

General statistical analyses

Statistical significance for biological samples was analyzed by applying Student's t test in pairwise comparisons, and one-way ANOVA corrected by Tukey HSD (alpha = 0.05) in the case of multiple group comparisons using GraphPad Prism version 8 (http://www.graphpad.com). If the number of samples (n) was more than three in each group, Shapiro-Wilk tests were performed to validate the normality of data distribution. The use of each test, as well as number of samples and replicates (technical and/or biological) if applicable, and p-value thresholds to account for statistical significance of each experiment are stated in the figure legend. Graphical depiction of center and dispersion per group sample represents mean and SD unless specified.

Quantification of dividing cells in EdU-labelled tissue

EdU-labelled nuclei were marked and counted with a modified version of the ITCN plugin[52] in ImageJ 1.52a[42]. Spatial coordinates for the nuclei were exported and processed with R scripts[53] to calculate density maps using the *spatstat* package[54]. Actively dividing area was measured as with nucleus densities higher than 0.001 μm^{-2}. See Key Resources Table for the repository of plugins and scripts used.

RNA sequencing data analyses

For RNA-seq data processing, reads from described sources were mapped to the *M. polymorpha* reference genome and quantified using Salmon 1.3.0 [55]. Reads from male lines were mapped to the MpTak1 v5.1 genome[56], while reads from female Mp*pif*^{ko} plants were mapped to autosome sequences from MpTak1 v5.1 plus the known U-chromosome scaffolds from genome ver 3.1 [11]. Differential gene expressions between sample pairs were analyzed with the R package DESeq2 [57], in which both autosome and V chromosome genes were considered for the Mp*DELLA* overexpression set, while only autosome genes were compared between Tak-1 and Mp*pif*^{ko}. Genes with a minimum fold change of 2 and adjusted p-value smaller than 0.01 were considered as significantly changed in expression. Compared with the wildtype, $_{pro}$*35S:*Mp*DELLA-Cit* led to the significant up- and down-regulation of 4 and 2 V-chromosome genes,

respectively. The total number of MpTak1 v5.1 autosome genes was used for checking if Mp*DELLA*-regulated genes were enriched in differentially expressed genes caused by Mp*pif*^{ko} using Fisher's exact test. UpSet plots were created using the R package ComplexHeatmap[58].

Fuzzy Gene Ontology (GO)[59] annotations for the v5.1 (plus ver 3.1 U-chromosome) genes were generated using the Blast2GO algorithm[60] written in R scripts. Briefly, all *M. polymorpha* reference proteins were blasted[61] against a database containing all UniProtKB[62] entries with non-IEA (inferred from electronic annotation) GO annotations, plus all Swiss-Prot entries (release 2020_05) with an e-value threshold of 0.001. Then the GO annotations from top 25 blast hits for each target protein were scored and concatenated based on their similarity and the GO hierarchy (release 2020-06-01). Annotations with scores higher than the user-defined thresholds (40 for cellular component, 55 for biological process, 50 for molecular function) were transferred to *M. polymorpha* proteins. GO enrichment analysis was conducted with biological process terms with the classic fisher's test from the *topGO* package[63]. R packages *GO.db*[64], *Rtsne*[65], *GOSemSim*[66,67], *rrvgo*[68] and *AnnotationForge*[69] were used for the clustering and visualization of top-enriched GO terms. Repositories for the raw sequence datasets, GO annotations and R scripts are listed in the Key Resources Table and the results are summarized in Data S1.

Metabolite profiling data processing

Processing of mass chromatograms was performed with xcms[70] after conversion to mzXML with MSConvert[71] using default settings. Chromatographic peak detection was performed using the matchedFilter algorithm, applying the following parameter settings: snr = 3, fwhm = 15 s, step = 0.01 D, mzdiff = 0.1 D, and profmethod = bin. Retention time correction was achieved in three iterations applying the parameter settings minfrac = 1, bw = 30 s, mzwid = 0.05D, span = 1, and missing = extra = 1 for the first iteration; minfrac = 1, bw = 10 s, mzwid = 0.05 D, span = 0.6, and missing = extra = 0 for the second iteration; and minfrac = 1, bw = 5 s, mzwid = 0.05 D, span = 0.5, and missing = extra = 0 for the third iteration. After final peak grouping (minfrac = 1, bw = 5 s) and filling in of missing features using the fillPeaks routine of the xcms package, a data matrix consisting

of feature × sample was obtained. When available, identification of metabolites was achieved by comparison of mass spectra and retention time with those of authentic standards or alternatively were tentatively annotated by matching experimental mass spectra in public databases (metlin, Massbank or HMDB). Known and temptative flavonoid-related compounds were chosen for comparison. Before statistical analyses, raw peak area values were normalized to internal standard area and sample weight. Pairwise comparisons were carried out using a two-tailed Student's t-test comparing two groups of samples of identical variance.

Supplemental Information

Data S1. RNA-seq expression profiles, GO annotations and top-enriched GO terms. Related to STAR Methods and Figure 3.

References

1. Thomas, S.G., Blázquez, M.A., and Alabadí, D. (2016). Della Proteins: Master Regulators of Gibberellin-Responsive Growth and Development. In Annual Plant Reviews: The Gibberellins, pp. 189–228.
2. Sun, T.P. (2011). The molecular mechanism and evolution of the GA-GID1-DELLA signaling module in plants. Curr. Biol. *21*, R338–R345.
3. Hedden, P., and Thomas, S.G. (2012). Gibberellin biosynthesis and its regulation. Biochem. J. *444*, 11–25.
4. Claeys, H., De Bodt, S., and Inze, D. (2014). Gibberellins and DELLAs: central nodes in growth regulatory networks. Trends Plant Sci *19*, 231–239.
5. Davière, J.-M., and Achard, P. (2016). A pivotal role of DELLAs in regulating multiple hormone signals. Mol. Plant *9*, 10–20.
6. Blázquez, M.A., Nelson, D.C., and Weijers, D. (2020). Evolution of Plant Hormone Response Pathways. Annu. Rev. Plant Biol. *71*, 327–353.
7. Hernández-García, J., Briones-Moreno, A., Dumas, R., and Blázquez, M.A. (2019). Origin of Gibberellin-Dependent Transcriptional Regulation by Molecular Exploitation of a Transactivation Domain in della Proteins. Mol. Biol. Evol. *36*, 908–918.

8. Hirano, K., Nakajima, M., Asano, K., Nishiyama, T., Sakakibara, H., Kojima, M., Katoh, E., Xiang, H., Tanahashi, T., Hasebe, M., et al. (2007). The GID1-mediated gibberellin perception mechanism is conserved in the lycophyte Selaginella moellendorffii but not in the bryophyte *Physcomitrella patens*. Plant Cell *19*, 3058–3079.
9. Yasumura, Y., Crumpton-Taylor, M., Fuentes, S., and Harberd, N.P. (2007). Step-by-Step Acquisition of the Gibberellin-DELLA Growth-Regulatory Mechanism during Land-Plant Evolution. Curr. Biol. *17*, 1225–1230.
10. Hernández-García, J., Briones-Moreno, A., and Blázquez, M.A. (2020). Origin and evolution of gibberellin signaling and metabolism in plants. Semin. Cell Dev. Biol. *109*, 46–54.
11. Bowman, J.L., Kohchi, T., Yamato, K.T., Jenkins, J., Shu, S., Ishizaki, K., Yamaoka, S., Nishihama, R., Nakamura, Y., Berger, F., et al. (2017). Insights into Land Plant Evolution Garnered from the Marchantia polymorpha Genome. Cell *171*, 287-304.e15.
12. Plackett, A.R.G., Thomas, S.G., Wilson, Z.A., and Hedden, P. (2011). Gibberellin control of stamen development: a fertile field. Trends Plant Sci. *16*, 568–578.
13. Itoh, H., Ueguchi-Tanaka, M., Sato, Y., Ashikari, M., and Matsuoka, M. (2002). The gibberellin signaling pathway is regulated by the appearance and disappearance of SLENDER RICE1 in nuclei. Plant Cell *14*, 57–70.
14. Silverstone, A.L., Jung, H.S., Dill, A., Kawaide, H., Kamiya, Y., and Sun, T.P. (2001). Repressing a repressor: gibberellin-induced rapid reduction of the RGA protein in Arabidopsis. Plant Cell *13*, 1555–1566.
15. Ikeda, A., Ueguchi-Tanaka, M., Sonoda, Y., Kitano, H., Koshioka, M., Futsuhara, Y., Matsuoka, M., and Yamaguchi, J. (2001). slender rice, a constitutive gibberellin response mutant, is caused by a null mutation of the SLR1 gene, an ortholog of the height-regulating gene GAI/RGA/RHT/D8. Plant Cell *13*, 999–1010.
16. Dill, A., Jung, H.-S., and Sun, T. (2001). The DELLA motif is essential for gibberellin-induced degradation of RGA. Proc. Natl. Acad. Sci. U. S. A. *98*, 14162–14167.
17. Peng, J., Richards, D.E., Hartley, N.M., Murphy, G.P., Devos, K.M.,

Flintham, J.E., Beales, J., Fish, L.J., Worland, A.J., Pelica, F., et al. (1999). “Green revolution” genes encode mutant gibberellin response modulators. Nature *400*, 256–261.

18. Martí, C., Orzáez, D., Ellul, P., Moreno, V., Carbonell, J., and Granell, A. (2007). Silencing of DELLA induces facultative parthenocarpy in tomato fruits. Plant J. *52*, 865–876.
19. Achard, P., Gusti, A., Cheminant, S., Alioua, M., Dhondt, S., Coppens, F., Beemster, G.T., and Genschik, P. (2009). Gibberellin signaling controls cell proliferation rate in Arabidopsis. Curr Biol *19*, 1188–1193.
20. Serrano-Mislata, A., Bencivenga, S., Bush, M., Schiessl, K., Boden, S., and Sablowski, R. (2017). DELLA genes restrict inflorescence meristem function independently of plant height. Nat. Plants *3*, 749–754.
21. Davière, J.M., Wild, M., Regnault, T., Baumberger, N., Eisler, H., Genschik, P., and Achard, P. (2014). Class I TCP-DELLA interactions in inflorescence shoot apex determine plant height. Curr. Biol. *24*, 1923–1928.
22. Ubeda-Tomás, S., Federici, F., Casimiro, I., Beemster, G.T.S., Bhalerao, R., Swarup, R., Doerner, P., Haseloff, J., and Bennett, M.J. (2009). Gibberellin Signaling in the Endodermis Controls Arabidopsis Root Meristem Size. Curr. Biol. *19*, 1194–1199.
23. Shani, E., Weinstain, R., Zhang, Y., Castillejo, C., Kaiserli, E., Chory, J., Tsien, R.Y., and Estelle, M. (2013). Gibberellins accumulate in the elongating endodermal cells of Arabidopsis root. Proc. Natl. Acad. Sci. U. S. A. *110*, 4834–4839.
24. Sugano, S.S., Nishihama, R., Shirakawa, M., Takagi, J., Matsuda, Y., Ishida, S., Shimada, T., Hara-Nishimura, I., Osakabe, K., and Kohchi, T. (2018). Efficient CRISPR/Cas9-based genome editing and its application to conditional genetic analysis in Marchantia polymorpha. PLoS One *13*, e0205117.
25. Inoue, K., Nishihama, R., Kataoka, H., Hosaka, M., Manabe, R., Nomoto, M., Tada, Y., Ishizaki, K., and Kohchi, T. (2016). Phytochrome signaling is mediated by PHYTOCHROME INTERACTING FACTOR in the liverwort *Marchantia polymorpha*. Plant Cell *28*, 1406–1421.
26. Inoue, K., Nishihama, R., Araki, T., and Kohchi, T. (2019). Reproductive

induction is a far-red high irradiance response that is mediated by phytochrome and PHYTOCHROME INTERACTING FACTOR in *Marchantia polymorpha*. Plant Cell Physiol. *60*, 1136–1145.

27. Gallego-Bartolomé, J., Arana, M. V., Vandenbussche, F., Žádníková, P., Minguet, E.G., Guardiola, V., Van Der Straeten, D., Benkova, E., Alabadí, D., and Blázquez, M.A. (2011). Hierarchy of hormone action controlling apical hook development in Arabidopsis. Plant J. *67*, 622–634.
28. De Lucas, M., Davière, J.M., Rodríguez-Falcón, M., Pontin, M., Iglesias-Pedraz, J.M., Lorrain, S., Fankhauser, C., Blázquez, M.A., Titarenko, E., and Prat, S. (2008). A molecular framework for light and gibberellin control of cell elongation. Nature *451*, 480–484.
29. Feng, S., Martinez, C., Gusmaroli, G., Wang, Y., Zhou, J., Wang, F., Chen, L., Yu, L., Iglesias-Pedraz, J.M., Kircher, S., et al. (2008). Coordinated regulation of *Arabidopsis thaliana* development by light and gibberellins. Nature *451*, 475–9.
30. Zhang, Y., Mayba, O., Pfeiffer, A., Shi, H., Tepperman, J.M., Speed, T.P., and Quail, P.H. (2013). A quartet of PIF bHLH factors provides a transcriptionally centered signaling hub that regulates seedling morphogenesis through differential expression-patterning of shared target genes in Arabidopsis. PLoS Genet *9*, e1003244.
31. Clayton, W.A., Albert, N.W., Thrimawithana, A.H., McGhie, T.K., Deroles, S.C., Schwinn, K.E., Warren, B.A., McLachlan, A.R.G., Bowman, J.L., Jordan, B.R., et al. (2018). UVR8-mediated induction of flavonoid biosynthesis for UVB tolerance is conserved between the liverwort Marchantia polymorpha and flowering plants. Plant J. *96*, 503–517.
32. Babbs, C.F., Pham, J.A., and Coolbaugh, R.C. (1989). Lethal Hydroxyl Radical Production in Paraquat-Treated Plants. Plant Physiol. *90*, 1267–1270.
33. Achard, P., Renou, J.P., Berthomé, R., Harberd, N.P., and Genschik, P. (2008). Plant DELLAs Restrain Growth and Promote Survival of Adversity by Reducing the Levels of Reactive Oxygen Species. Curr. Biol. *18*, 656–660.
34. Ishizaki, K., Chiyoda, S., Yamato, K.T., and Kohchi, T. (2008). *Agrobacterium*-mediated transformation of the haploid liverwort

Marchantia polymorpha L., an emerging model for plant biology. Plant Cell Physiol. *49*, 1084–1091.

35. Gamborg, O.L., Miller, R.A., and Ojima, K. (1968). Nutrient requirements of suspension cultures of soybean root cells. Exp. Cell Res. *50*, 151–158.
36. Ishizaki, K., Nishihama, R., Ueda, M., Inoue, K., Ishida, S., Nishimura, Y., Shikanai, T., and Kohchi, T. (2015). Development of gateway binary vector series with four different selection markers for the liverwort marchantia polymorpha. PLoS One.
37. Sugano, S.S., Shirakawa, M., Takagi, J., Matsuda, Y., Shimada, T., Hara-Nishimura, I., and Kohchi, T. (2014). CRISPR/Cas9-mediated targeted mutagenesis in the liverwort *Marchantia polymorpha* L. Plant Cell Physiol. *55*, 475–481.
38. Benchling [Biology Software] (2021).
39. Kubota, A., Ishizaki, K., Hosaka, M., and Kohchi, T. (2013). Efficient *Agrobacterium*-mediated transformation of the liverwort *Marchantia polymorpha* using regenerating thalli. Biosci. Biotechnol. Biochem. *77*, 167–172.
40. Koncz, C., and Schell, J. (1986). The promoter of TL-DNA gene 5 controls the tissue-specific expression of chimaeric genes carried by a novel type of Agrobacterium binary vector. MGG Mol. Gen. Genet. *204*.
41. Deblaere, R., Bytebier, B., De Greve, H., Deboeck, F., Schell, J., Van Montagu, M., and Leemans, J. (1985). Efficient octopine Ti plasmid-derived vectors for Agrobacterium -mediated gene transfer to plants. Nucleic Acids Res. *13*, 4777–4788.
42. Schneider, C.A., Rasband, W.S., and Eliceiri, K.W. (2012). NIH Image to ImageJ: 25 years of image analysis. Nat. Methods *9*, 671–675.
43. Kurihara, D., Mizuta, Y., Sato, Y., and Higashiyama, T. (2015). ClearSee: A rapid optical clearing reagent for whole-plant fluorescence imaging. Development *142*, 4168–4179.
44. Peer, W.A., Brown, D.E., Tague, B.W., Muday, G.K., Taiz, L., and Murphy, A.S. (2001). Flavonoid accumulation patterns of transparent *testa* mutants of Arabidopsis. Plant Physiol. *126*, 536–548.
45. Rossignol, P., Collier, S., Bush, M., Shaw, P., and Doonan, J.H. (2007). Arabidopsis POT1A interacts with TERT-V(18), an N-terminal splicing

variant of telomerase. J. Cell Sci. *120*, 3678–3687.

46. Gietz, R.D., and Woods, R.A. (2002). Transformation of yeast by lithium acetate/single-stranded carrier DNA/polyethylene glycol method. Methods Enzymol. *350*, 87–96.
47. Earley, K.W., Haag, J.R., Pontes, O., Opper, K., Juehne, T., Song, K., and Pikaard, C.S. (2006). Gateway-compatible vectors for plant functional genomics and proteomics. Plant J. *45*, 616–629.
48. Belda-Palazón, B., Ruiz, L., Martí, E., Tárraga, S., Tiburcio, A.F., Culiáñez, F., Farràs, R., Carrasco, P., and Ferrando, A. (2012). Aminopropyltransferases Involved in Polyamine Biosynthesis Localize Preferentially in the Nucleus of Plant Cells. PLoS One *7*.
49. Marín-de la Rosa, N., Pfeiffer, A., Hill, K., Locascio, A., Bhalerao, R.P., Miskolczi, P., Grønlund, A.L., Wanchoo-Kohli, A., Thomas, S.G., Bennett, M.J., et al. (2015). Genome Wide Binding Site Analysis Reveals Transcriptional Coactivation of Cytokinin-Responsive Genes by DELLA Proteins. PLoS Genet. *11*, 1–20.
50. Hellemans, J., Mortier, G., De Paepe, A., Speleman, F., and Vandesompele, J. (2008). qBase relative quantification framework and software for management and automated analysis of real-time quantitative PCR data. Genome Biol. *8*.
51. Zandalinas, S.I., Sales, C., Beltrán, J., Gómez-Cadenas, A., and Arbona, V. (2017). Activation of Secondary Metabolism in Citrus Plants Is Associated to Sensitivity to Combined Drought and High Temperatures. Front. Plant Sci. *7*, 1954.
52. Kuo, T., and Byun, J. ITCN: Image-based Tool for Counting Nuclei.
53. R-Core-Team (2020). R: A language and environment for statistical computing. R Foundation for Statistical Computing.
54. Baddeley, A., and Turner, R. (2005). spatstat: An R package for analyzing spatial point patterns. J. Stat. Softw. *12*, 1–42.
55. Patro, R., Duggal, G., Love, M.I., Irizarry, R.A., and Kingsford, C. (2017). Salmon provides fast and bias-aware quantification of transcript expression. Nat. Methods *14*, 417–419.
56. Montgomery, S.A., Tanizawa, Y., Galik, B., Wang, N., Ito, T., Mochizuki, T., Akimcheva, S., Bowman, J.L., Cognat, V., Maréchal-Drouard, L., et al.

(2020). Chromatin Organization in Early Land Plants Reveals an Ancestral Association between H3K27me3, Transposons, and Constitutive Heterochromatin. Curr. Biol. *30*, 573-588.e7.

57. Love, M.I., Huber, W., and Anders, S. (2014). Moderated estimation of fold change and dispersion for RNA-seq data with DESeq2. Genome Biol. *15*, 550.
58. Gu, Z., Eils, R., and Schlesner, M. (2016). Complex heatmaps reveal patterns and correlations in multidimensional genomic data. Bioinformatics *32*, 2847–2849.
59. The Gene Ontology resource: enriching a GOld mine (2021). Nucleic Acids Res.
60. Götz, S., García-Gómez, J.M., Terol, J., Williams, T.D., Nagaraj, S.H., Nueda, M.J., Robles, M., Talón, M., Dopazo, J., and Conesa, A. (2008). High-throughput functional annotation and data mining with the Blast2GO suite. Nucleic Acids Res. *36*, 3420–3435.
61. Camacho, C., Coulouris, G., Avagyan, V., Ma, N., Papadopoulos, J., Bealer, K., and Madden, T.L. (2009). BLAST+: Architecture and applications. BMC Bioinformatics.
62. The Uniprot Consortium, . (2019). UniProt: a worldwide hub of protein knowledge The UniProt Consortium. Nucleic Acids Res.
63. Alexa, A., and Rahnenfuhrer, J. (2020). topGO: Enrichment Analysis for Gene Ontology. R Packag. version 2.42.0.
64. Carlson, M. (2019). GO.db: A set of annotation maps describing the entire Gene Ontology. R Packag. version 3.8.2.
65. Krijthe, J.H. (2015). Rtsne: T-Distributed Stochastic Neighbor Embedding using a Barnes-Hut Implementation.
66. Yu, G., Li, F., Qin, Y., Bo, X., Wu, Y., and Wang, S. (2010). GOSemSim: an R package for measuring semantic similarity among GO terms and gene products. Bioinformatics *26*, 976–978.
67. Yu, G. (2020). Gene ontology semantic similarity analysis using GOSemSim. In Methods in Molecular Biology (Humana Press Inc.), pp. 207–215.
68. Sayols, S. (2020). rrvgo: a Bioconductor package to reduce and visualize Gene Ontology terms.

69. Carlson, M., and Pagès, H. (2020). AnnotationForge: Tools for building SQLite-based annotation data packages. R Packag. version 1.32.0.
70. Smith, C.A., Want, E.J., O'Maille, G., Abagyan, R., and Siuzdak, G. (2006). XCMS: Processing mass spectrometry data for metabolite profiling using nonlinear peak alignment, matching, and identification. Anal. Chem. *78*, 779–787.
71. Chambers, M.C., MacLean, B., Burke, R., Amodei, D., Ruderman, D.L., Neumann, S., Gatto, L., Fischer, B., Pratt, B., Egertson, J., et al. (2012). A cross-platform toolkit for mass spectrometry and proteomics. Nat. Biotechnol. *30*, 918–920.

KEY RESOURCES TABLE

REAGENT or RESOURCE	SOURCE	IDENTIFIER
Antibodies		
Anti-GFP JL-8	Takara Bio	Cat#632380
Anti-HA-Peroxidase, High Affinity (3F10)	Sigma-Aldrich	Cat#12013819001
Goat anti-Mouse IgM (Heavy Chain) Secondary Antibody, HRP	Thermo Fisher Scientific	Cat#626820
Bacterial and Virus Strains		
Escherichia coli DH5α	Widely distributed	N/A
Escherichia coli TOP10	Widely distributed	N/A
Agrobacterium tumefaciens GV3101 (pMP90 C58)	[40]	N/A
Agrobacterium tumefaciens GV2260	[41]	N/A
Chemicals, Peptides, and Recombinant Proteins		
Gamborg's B5 salts	[35]	N/A
Chlorsulfuron	Sigma-Aldrich	Cat#N11461
Chlorsulfuron (Glean XP)	Dupont	EPA#352-653
Hygromycin B	PanReac AppliChem	Cat#A2175-0005
Hygromycin B	Nacalai Tesque	Cat#07296-24
Cefotaxime sodium	Duchefa Biochemie	Cat#C0111.0005
Cefotaxime (CLAFORAN)	Sanofi	Cat#6132409D1050
3,5-Dimethoxy-4-hydroxyacetophenone (Acetosyringone)	Sigma-Aldrich	Cat#D134406
Dexamethasone (DEX)	Sigma-Aldrich	Cat#D4902
Dexamethasone (DEX)	Fujifilm Wako	Cat#041-18861
Albumin, bovine (BSA)	Nacalai Tesque	Cat#08777-36
3-Amino-1,2,4-triazole	Sigma-Aldrich	Cat#A8056-100G
Methyl viologen dichloride hydrate	Sigma-Aldrich	Cat#856177
5-bromo-4-chloro-3-indolyl-β-D-glucuronic acid (X-Gluc)	Carbosynth	Cat#B-7300
Diphenylboric acid 2-aminoethyl ester (DPBA)	Sigma-Aldrich	Cat#358835
MG-132 in Solution	Calbiochem	Cat#474791
cOmplete Protease Inhibitor Cocktail	Sigma-Aldrich	Cat#05056489001
Phenylmethylsulfonyl fluoride (PMSF)	Sigma-Aldrich	Cat#P7626-1G
Biochanin A	Sigma Aldrich	Cat#D2016
LC/MS grade methanol	Fisher Scientific	Cat#A456-212
LC/MS grade acetonitrile	Fisher Scientific	Cat#A/0638/17
LC/MS grade formic acid	Fisher Scientific	Cat#A117-50
Critical Commercial Assays		
Phusion High-Fidelity Polymerase	Thermo Fisher Scientific	Cat#F530L
KOD FX Neo DNA polymerase	Toyobo Life Science	Cat#KFX-201
KOD -Plus- Ver.2 DNA polymerase	Toyobo Life Science	Cat#KOD-211
PrimeSTAR GXL DNA Polymerase	TaKaRa Bio	Cat#R050A
pENTR/D-TOPO Cloning Kit	Thermo Fisher Scientific	Cat#K2400-20
pCR8/GW/TOPO TA Cloning Kit	Thermo Fisher Scientific	Cat#K2500-20
In-Fusion HD Cloning Kit	TaKaRa Bio	Cat#639649
Bsa I	New England Biolabs	Cat#R0535L

*Eco*R V	TaKaRa Bio	Cat#1042A
Not I	TaKaRa Bio	Cat#1166A
Sal I	TaKaRa Bio	Cat#1080A
T4 DNA ligase	Promega	Cat#M1804
T4 DNA ligase	TaKaRa Bio	Cat#2011A
Ligation high Ver.2 DNA ligase	Toyobo Life Science	Cat#LGK-201
Gateway BP Clonase II Enzyme mix	Thermo Fisher Scientific	Cat#11789-020
Gateway LR Clonase II Enzyme mix	Thermo Fisher Scientific	Cat#11791-020
Click-iT EdU Alexa Fluor 488 Imaging Kit	Invitrogen	Cat#C10337
Protein Assay Dye Reagent Concentrate	BIO-RAD	Cat#500-0006
µMACS GFP Isolation Kit	Miltenyi Biotec	Cat#130-091-125
SuperSignal West FEMTO maximum sensitivity substrate	Thermo Fisher Scientific	Cat#34095
Dual-Glo Luciferase Assay System	Promega	Cat#E2920
TRIzol Reagent	Invitrogen	Cat#15596018
RNeasy Plant Mini Kit	QIAGEN	Cat#74904
RNeasy MinElute Cleanup Kit	QIAGEN	Cat#74204
RQ1 RNase-Free DNase	Promega	Cat#M6101
RNase-free DNase Set Kit	QIAGEN	Cat#74254
ReverTra Ace	Toyobo Life Science	Cat#TRT-101
PrimeScript 1st strand cDNA Synthesis Kit	Takara Bio	Cat#6110A
TaKaRa Ex Taq	Takara Bio	Cat#RR001A
SYBR Green I Nucleic Acid Stain	Lonza	Cat#50513
SYBR Premix Ex Taq	Takara Bio	Cat#RR420W
Bioanalyzer RNA6000 Nano Kit	Agilent Technologies	Cat#5067-1511
Qubit RNA HS Assay Kit	Thermo Fisher Scientific	Cat#Q32852
TruSeq RNA Library Prep Kit v2	Illumina	Cat#RS-122-2001
KAPA Library Quantification Kit	Roche	Cat#KK4824
Luna Omega 1.6 mm Polar C18 100 x 2.1 mm	Phenomenex	Cat#00D-4748-AN
Cytiva Whatman Qualitative Filter Paper: Grade 1 Circles	Fisher Scientific	Cat#10738611
Deposited Data		
Mp*DELLA* overexpression RNA-seq data	this paper	NCBI Bioproject #PRJNA695248
Mp*pif*^{ko} with far-red irradiation RNA-seq data	this paper	DDBJ Bioproject #PRJDB11176
Experimental Models: Organisms/Strains		
Saccharomyces cerevisiae: Y2HGold	Takara Bio	Cat#630498
Saccharomyces cerevisiae: Y187	Takara Bio	Cat#630457
Nicotiana benthamiana lab strain	Widely distributed	N/A
Marchantia polymorpha: Tak-1	[34]	N/A
Marchantia polymorpha: pif^{ko} #1	[25]	N/A
Marchantia polymorpha: gPIF/pif^{ko} #1	[25]	N/A
Marchantia polymorpha: Tak-1 $_{pro}$*35S*:Mp*DELLA-Citrine* (Tak-1/ pMpGWB106) #2	This paper	N/A
Marchantia polymorpha: Tak-1 $_{pro}$M*pEF1α*:Mp*DELLA-3xFLAG* (pMpGWB310) #1	This paper	N/A

Marchantia polymorpha: Tak-1 $_{pro}$Mp*EF1α*:Mp*DELLA-3xFLAG* (pMpGWB310) #5	This paper	N/A
Marchantia polymorpha: Tak-1 *g*Mp*DELLA-GUS* (pMpGWB304) #1	This paper	N/A
Marchantia polymorpha: Tak-1 *g*Mp*DELLA-GUS* (pMpGWB304) #2	This paper	N/A
Marchantia polymorpha: Tak-1 $_{pro}$Mp*DELLA:GUS* (pMpGWB304)	This paper	N/A
Marchantia polymorpha: Tak-1 *g*Mp*DELLA-Citrine* (pMpGWB307) #1	This paper	N/A
Marchantia polymorpha: Tak-1 $_{pro}$Mp*EF1α*:Mp*DELLA-GR* (pMpGWB313) #4	This paper	N/A
Marchantia polymorpha: Tak-1 $_{pro}$Mp*EF1α*:Mp*DELLA-GR* (pMpGWB313) #5	This paper	N/A
Marchantia polymorpha: $_{pro}$Mp*EF1α*:Mp*DELLA-GR* (pMpGWB313) #5; $_{pro}$Mp*CYCB;1:Dbox-GUS* (pMpGWB104) #19	This paper	N/A
Marchantia polymorpha: $_{pro}$Mp*EF1α*:Mp*DELLA-GR* (pMpGWB313) #5; $_{pro}$Mp*CYCB;1:Dbox-GUS* (pMpGWB104) #32	This paper	N/A
Marchantia polymorpha: $_{pro}$Mp*EF1α*:Mp*DELLA-GR* (pMpGWB313) #5; Mp*smr*$^{ge-1}$ (pMpGE010)	This paper	N/A
Marchantia polymorpha: $_{pro}$Mp*EF1α*:Mp*DELLA-GR* (pMpGWB313) #5; Mp*smr*$^{ge-2}$ (pMpGE010)	This paper	N/A
Marchantia polymorpha: $_{pro}$Mp*EF1α*:Mp*DELLA-GR* (pMpGWB313) #5; $_{pro}$*35S:Citrine*-Mp*PIF* (pMpGWB105) #2	This paper	N/A
Marchantia polymorpha: $_{pro}$Mp*EF1α*:Mp*DELLA-GR* (pMpGWB313) #5; $_{pro}$*35S:Citrine*-Mp*PIF* (pMpGWB105) #1	This paper	N/A
Marchantia polymorpha: $_{pro}$Mp*EF1α*:Mp*DELLA-GR* (pMpGWB313) #5; $_{pro}$*35S:Citrine*-Mp*PIF* (pMpGWB105) #2	This paper	N/A
Marchantia polymorpha: $_{pro}$Mp*EF1α*:Mp*DELLA-GR* (pMpGWB313) #5; $_{pro}$*35S:Citrine*-Mp*PIF* (pMpGWB105) #8	This paper	N/A
Oligonucleotides		
See Table S1 for primers	This paper	N/A
Recombinant DNA		
pDONR221	Thermo Fisher Scientific	Cat#12536017
pENTR221-MpDELLA	This paper	N/A
pENTR221-MpDELLA^{GRAS}	This paper	N/A
pENTR221-$_{pro}$MpDELLA	This paper	N/A
pENTR221-gMpDELLA	This paper	N/A
pENTR/D-TOPO	Thermo Fisher Scientific	Cat#K2400-20
pENTR-MpDELLA	This paper	N/A
pENTR-MpPIF-Stop	This paper	N/A
pENTR1A	Thermo Fisher Scientific	Cat#A10462
pENTR1A-$_{pro}$MpDELLA-short	This paper	N/A
pENTR1A-gMpDELLA-short	This paper	N/A

pENTR1A-$_{pro}$MpDELLA	This paper	N/A
pENTR1A-gMpDELLA	This paper	N/A
pENTR1A-$_{pro}$MpCYCB;1-Dbox	This paper	N/A
pCR8/GW/TOPO	Thermo Fisher Scientific	Cat#K2500-20
pCR8-MpPIF	This paper	N/A
pCR8-MpPIFdel1	This paper	N/A
pCR8-MpPIFdel2	This paper	N/A
pCR8-MpPIFdel3	This paper	N/A
pCR8-MpPIFdel4	This paper	N/A
pMpGWB104	[36]	Addgene #68558
pMpGWB104-$_{pro}$MpCYCB;1-Dbox	This paper	N/A
pMpGWB105	[36]	Addgene #68559
pMpGWB105-MpPIF	This paper	N/A
pMpGWB106	[36]	Addgene #68560
pMpGWB106-MpDELLA	This paper	N/A
pMpGWB304	[36]	Addgene #68632
pMpGWB304-$_{pro}$MpDELLA	This paper	N/A
pMpGWB304-gMpDELLA	This paper	N/A
pMpGWB307	[36]	Addgene #68635
pMpGWB307-gMpDELLA	This paper	N/A
pMpGWB310	[36]	Addgene #68638
pMpGWB310-MpDELLA	This paper	N/A
pMpGWB313	[36]	Addgene #68641
pMpGWB313-MpDELLA	This paper	N/A
pMpGE_En03	[36]	Addgene #71535
pMpGE_En03-MpDELLA-sgV01	This paper	N/A
pMpGE_En03-MpDELLA-sgV02	This paper	N/A
pMpGE_En03-MpDELLA-sgV03	This paper	N/A
pMpGE_En03-MpDELLA-sgK01	This paper	N/A
pMpGE_En03-MpDELLA-sgK02	This paper	N/A
pMpGE_En03-MpDELLA-sgK03	This paper	N/A
pMpGE_En03-MpDELLA-sgK04	This paper	N/A
pMpGE_En03-MpSMR-sgRNA	This paper	N/A
pMpGE010	[36]	Addgene #71536
pMpGE010-MpDELLA-sgV01	This paper	N/A
pMpGE010-MpDELLA-sgV02	This paper	N/A
pMpGE010-MpDELLA-sgV03	This paper	N/A
pMpGE010-MpDELLA-sgK01	This paper	N/A
pMpGE010-MpDELLA-sgK02	This paper	N/A
pMpGE010-MpDELLA-sgK03	This paper	N/A
pMpGE010-MpDELLA-sgK04	This paper	N/A
pMpGE010-MpSMR-sgRNA	This paper	N/A
pGADT7-GW	[45]	N/A
pGADT7-MpPIF	This paper	N/A
pGADT7-MpPIFdel1	This paper	N/A
pGADT7-MpPIFdel2	This paper	N/A
pGADT7-MpPIFdel3	This paper	N/A

pGADT7-MpPIFdel4	This paper	N/A
pGBKT7-GW	[45]	N/A
pGBKT7-MpDELLA^{GRAS}	This paper	N/A
pEarleyGate104	[47]	N/A
pEarleyGate104-MpDELLA	This paper	N/A
pEarleyGate201	[47]	N/A
pEarleyGate201-MpPIF	This paper	N/A
pEarleyGate201-MpPIFdel3	This paper	N/A
pGreenII 0800 pAtPIL1:LUC	[30]	N/A
35S:p19	Widely distributed	N/A
pMDC43-YFN	[48]	N/A
pMDC43-YFN-MpDELLA	This paper	N/A
pMDC43-YFC	[48]	N/A
pMDC43-YFC-MpPIF	This paper	N/A
Software and Algorithms		
Benchling	[38]	https://benchling.com
Prism 8	GraphPad Software	http://www.graphpad.com
BZ-X Analyzer	Keyence	N/A
ImageJ	[42]	https://imagej.nih.gov/ij/
ITCN plugin for ImageJ	[52]	https://bioimage.ucsb.edu/docs/automatic-nuclei-counter-plugin-imagej
Modified ITCN plugin for ImageJ	This paper	https://github.com/PMB-KU/CountNuclei
Salmon 1.3.0	[55]	https://combine-lab.github.io/salmon/
Blast2GO algorithm	[60]	https://www.blast2go.com
R version 4.0.3	[53]	http://www.R-project.org
R package *spatstat* 1.64-1	[54]	http://www.spatstat.org
R package *DESeq2* 1.30.0	[57]	https://github.com/mikelove/DESeq2
R package *topGO* 2.42.0	[63]	https://bioconductor.org/packages/release/bioc/html/topGO.html
R package *GO.db* 3.12.1	[64]	https://bioconductor.org/packages/release/data/annotation/html/GO.db.html
R package Rtsne 0.15	[65]	https://github.com/jkrijthe/Rtsne
R package *GOSemSim* 2.16.1	[66, 67]	https://guangchuangyu.github.io/software/GOSemSim

R package *rrvgo* 1.2.0	[68]	https://ssayols.github.io/rrvgo
R package *AnnotationForge* 1.32.0	[69]	https://bioconductor.org/packages/AnnotationForge
xcms	[70]	https://xcmsonline.scripps.edu
MSConvert in ProteoWizard	[71]	http://proteowizard.sourceforge.net
Other		
Scripts used for EdU analysis, RNA-seq analysis, GO annotation & visualization	This paper	https://github.com/dorrenasun/MpDELLA

Figure 1

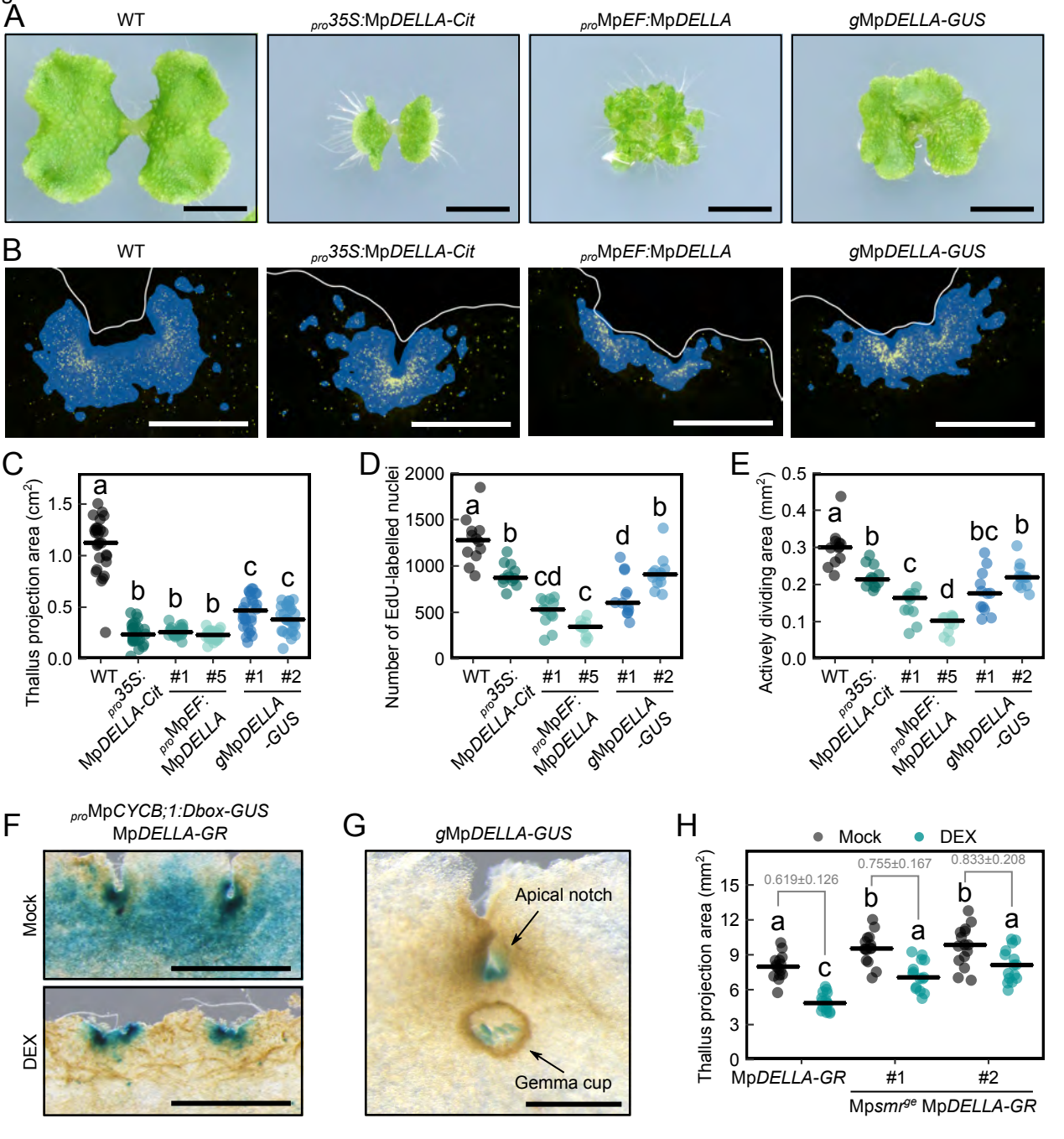
A
WT
proMpEF:MpDELLA
gMpDELLA-GUS
B
WT
proMpEF:MpDELLA
gMpDELLA-GUS
C
Thallus projection area (cm2)
WT
#1
#5
#1
#2
gMpDELLA-GUS
D
Number of EdU-labelled nuclei
WT
#1
#5
#1
#2
gMpDELLA-GUS
E
Actively dividing area (mm2)
WT
#1
#5
#1
#2
gMpDELLA-GUS
F
proMpCYCB;1:Dbox-GUS
MpDELLA-GR
Mock
DEX
G
gMpDELLA-GUS
Apical notch
Gemma cup
H
Mock
DEX
0.619±0.126
0.755±0.167
0.833±0.208
Thallus projection area (mm2)
MpDELLA-GR
#1
#2
Mpsmge MpDELLA-GR

Figure 2

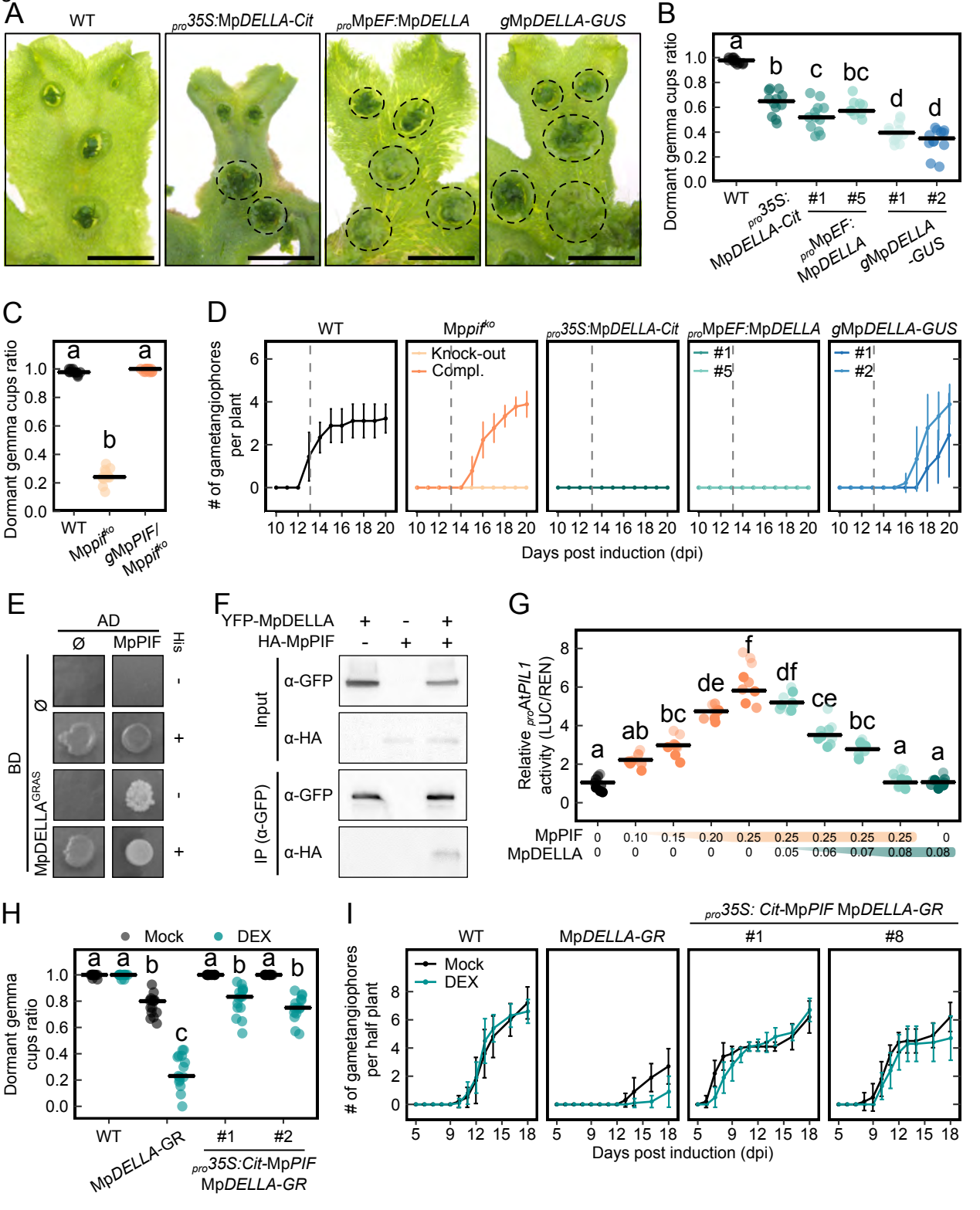
A
WT
pro35S:MpDELLA-Cit
proMpEF:MpDELLA
gMpDELLA-GUS
B
Dormant gemma cups ratio
WT
pro35S: MpDELLA-Cit
proMpEF: MpDELLA #1
proMpEF: MpDELLA #5
gMpDELLA -GUS #1
gMpDELLA -GUS #2
C
Dormant gemma cups ratio
WT
Mppif ko
gMpPIF/ Mppif ko
D
WT
Mppif ko
Knock-out
Compl.
pro35S:MpDELLA-Cit
proMpEF:MpDELLA
gMpDELLA-GUS
# of gametangiophores per plant
Days post induction (dpi)
E
AD
Ø
MpPIF
His
BD
Ø
MpDELLA GRAS
F
YFP-MpDELLA
HA-MpPIF
Input
IP (α-GFP)
α-GFP
α-HA
G
Relative proAtPIL1 activity (LUC/REN)
MpPIF
MpDELLA
H
Mock
DEX
Dormant gemma cups ratio
WT
MpDELLA-GR
pro35S:Cit-MpPIF MpDELLA-GR #1
pro35S:Cit-MpPIF MpDELLA-GR #2
I
WT
MpDELLA-GR
pro35S: Cit-MpPIF MpDELLA-GR
#1
#8
Mock
DEX
# of gametangiophores per half plant
Days post induction (dpi)

Figure 3

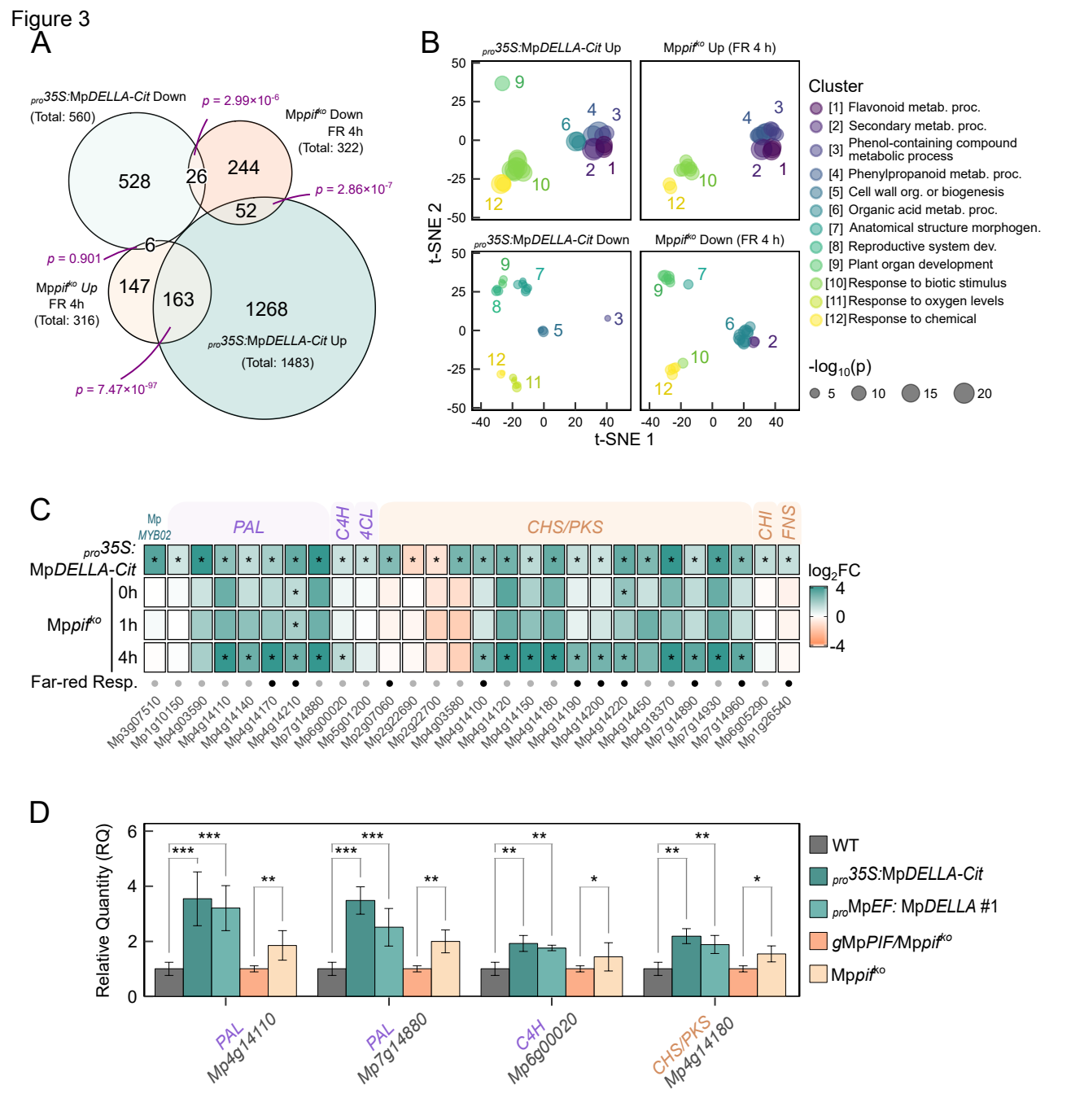
A
pro35S:MpDELLA-Cit Down
(Total: 560)
p = 2.99×10-6
Mppifko Down
FR 4h
(Total: 322)
528
26
244
p = 2.86×10-7
52
p = 0.901
6
Mppifko Up
FR 4h
(Total: 316)
147
163
1268
pro35S:MpDELLA-Cit Up
(Total: 1483)
p = 7.47×10-97
B
pro35S:MpDELLA-Cit Up
Mppifko Up (FR 4 h)
pro35S:MpDELLA-Cit Down
Mppifko Down (FR 4 h)
t-SNE 2
t-SNE 1
Cluster
[1] Flavonoid metab. proc.
[2] Secondary metab. proc.
[3] Phenol-containing compound metabolic process
[4] Phenylpropanoid metab. proc.
[5] Cell wall org. or biogenesis
[6] Organic acid metab. proc.
[7] Anatomical structure morphogen.
[8] Reproductive system dev.
[9] Plant organ development
[10] Response to biotic stimulus
[11] Response to oxygen levels
[12] Response to chemical
-log10(p)
5
10
15
20
C
Mp MYB02
PAL
C4H
4CL
CHS/PKS
CHI
FNS
pro35S: MpDELLA-Cit
Mppifko
0h
1h
4h
Far-red Resp.
log2FC
4
0
-4
Mp3g07510
Mp1g10150
Mp4g03590
Mp4g14110
Mp4g14140
Mp4g14170
Mp4g14210
Mp7g14880
Mp6g00020
Mp5g01200
Mp2g07060
Mp2g22690
Mp2g22700
Mp4g03580
Mp4g14100
Mp4g14120
Mp4g14150
Mp4g14180
Mp4g14190
Mp4g14200
Mp4g14220
Mp4g14450
Mp4g18370
Mp7g14890
Mp7g14930
Mp7g14960
Mp6g05290
Mp1g26540
D
Relative Quantity (RQ)
WT
pro35S:MpDELLA-Cit
proMpEF: MpDELLA #1
gMpPIF/Mppifko
Mppifko
PAL Mp4g14110
PAL Mp7g14880
C4H Mp6g00020
CHS/PKS Mp4g14180

Figure 4

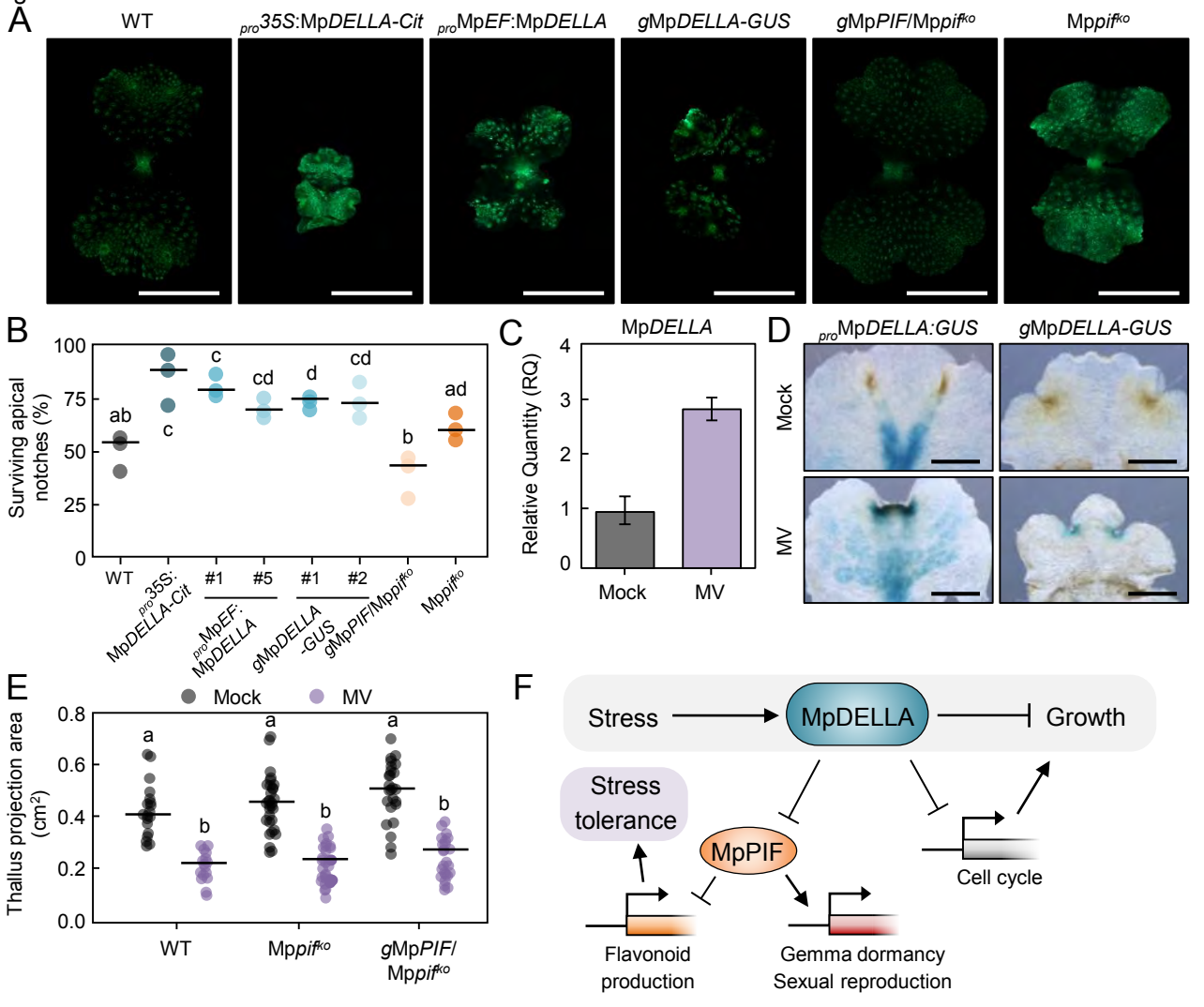
A
WT
pro35S:MpDELLA-Cit
proMpEF:MpDELLA
gMpDELLA-GUS
gMpPIF/Mppifko
Mppifko
B
Surviving apical notches (%)
ab
c
c
cd
d
cd
b
ad
WT
pro35S: MpDELLA-Cit
proMpEF: MpDELLA #1
#5
gMpDELLA -GUS #1
#2
gMpPIF/Mppifko
Mppifko
C
MpDELLA
Relative Quantity (RQ)
Mock
MV
D
proMpDELLA:GUS
gMpDELLA-GUS
Mock
MV
E
Mock
MV
Thallus projection area (cm2)
a
b
a
b
a
b
WT
Mppifko
gMpPIF/ Mppifko
F
Stress
MpDELLA
Growth
Stress tolerance
MpPIF
Cell cycle
Flavonoid production
Gemma dormancy
Sexual reproduction

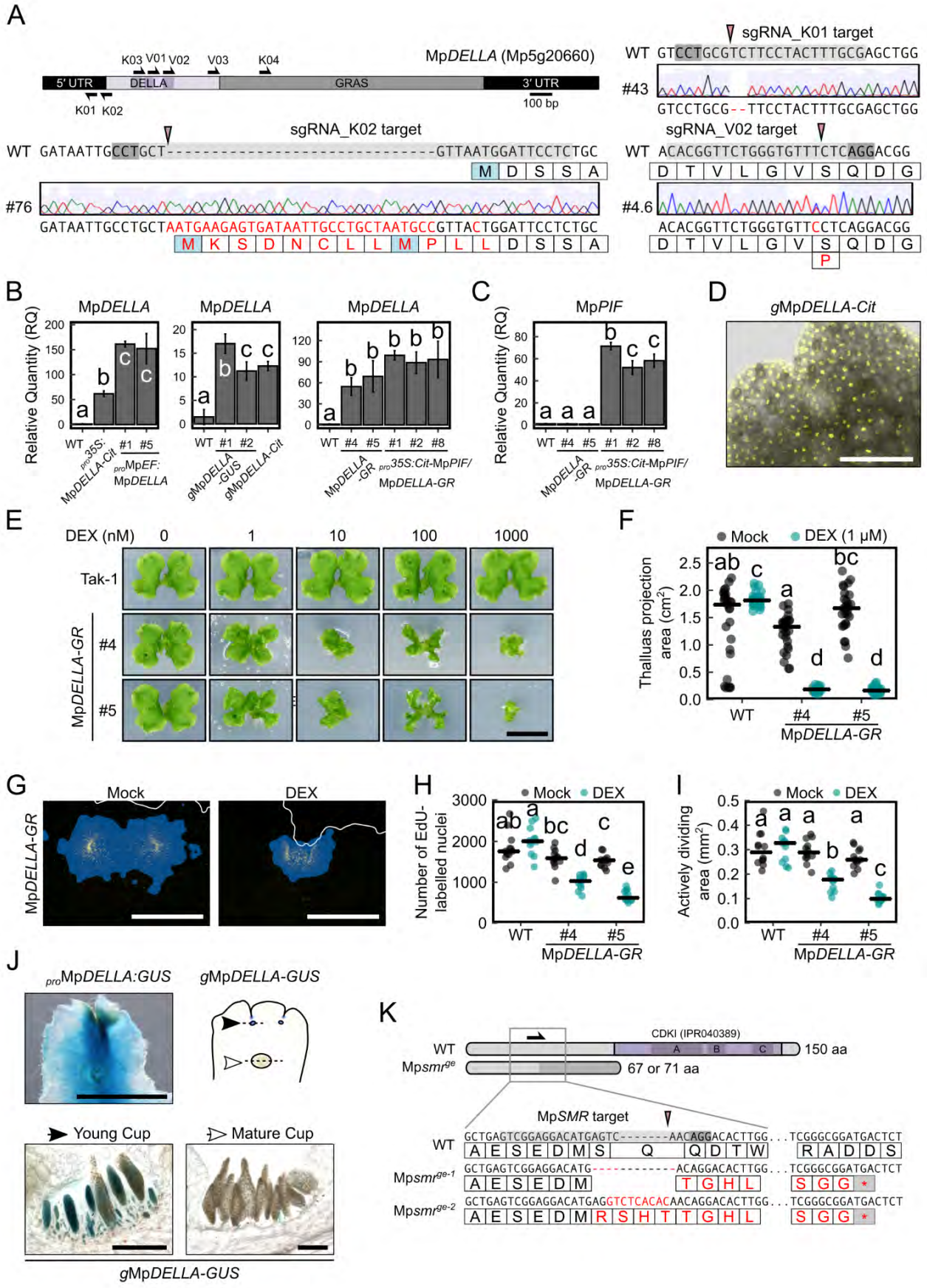
A
MpDELLA (Mp5g20660)
5′ UTR
DELLA
GRAS
3′ UTR
100 bp
K01 K02
K03 V01 V02
V03
K04
sgRNA_K01 target
WT GTCCTGCGTCTTCCTACTTTGCGAGCTGG
#43
GTCCTGCG--TTCCTACTTTGCGAGCTGG
sgRNA_K02 target
WT GATAATTGCCTGCT----------GTTAATGGATTCCTCTGC
M D S S A
#76
GATAATTGCCTGCTAATGAAGAGTGATAATTGCCTGCTAATGCCGTTACTGGATTCCTCTGC
M K S D N C L L M P L L D S S A
sgRNA_V02 target
WT ACACGGTTCTGGGTGTTTCTCAGGACGG
D T V L G V S Q D G
#4.6
ACACGGTTCTGGGTGTTCCTCAGGACGG
D T V L G V S Q D G
P
B
MpDELLA
Relative Quantity (RQ)
WT pro35S:MpDELLA-Cit #1 #5 proMpEF:MpDELLA
WT #1 #2 gMpDELLA-GUS gMpDELLA-Cit
WT #4 #5 #1 #2 #8 MpDELLA-GR pro35S:Cit-MpPIF/MpDELLA-GR
C
MpPIF
Relative Quantity (RQ)
WT #4 #5 #1 #2 #8 MpDELLA-GR pro35S:Cit-MpPIF/MpDELLA-GR
D
gMpDELLA-Cit
E
DEX (nM) 0 1 10 100 1000
Tak-1
MpDELLA-GR
#4
#5
F
Mock
DEX (1 μM)
Thallus projection area (cm²)
WT #4 #5 MpDELLA-GR
G
Mock
DEX
MpDELLA-GR
H
Mock DEX
Number of EdU-labelled nuclei
WT #4 #5 MpDELLA-GR
I
Mock DEX
Actively dividing area (mm²)
WT #4 #5 MpDELLA-GR
J
proMpDELLA:GUS
gMpDELLA-GUS
Young Cup
Mature Cup
gMpDELLA-GUS
K
CDKI (IPR040389)
A B C
WT 150 aa
Mpsmge 67 or 71 aa
MpSMR target
WT GCTGAGTCGGAGGACATGAGTC-------AACAGGACACTTGG...TCGGGCGGATGACTCT
A E S E D M S Q Q D T W R A D D S
Mpsmge-1 GCTGAGTCGGAGGACATG----------ACAGGACACTTGG...TCGGGCGGATGACTCT
A E S E D M T G H L S G G *
Mpsmge-2 GCTGAGTCGGAGGACATGAGTCTCACACAACAGGACACTTGG...TCGGGCGGATGACTCT
A E S E D M R S H T T G H L S G G *

Figure S1. Characterization of transgenic lines involving MpDELLA. Related to Figure 1.

(A) CRISPR-Cas9 genome editing attempts to obtain a Mp*della* mutant. Positions of short guide RNA (sgRNA) targets designed independently in Kyoto (K) or Valencia (V) were indicated in the illustration, and chromatograms showed sequencing data for three mutations obtained. #76 from sgRNA_K02 changed the sequences around the start codon but caused no frameshifts. sgRNA_V02 generated the 1-bp substitution in #4.3 in a chimeric manner and was eventually taken over by the wild-type tissue. The 2-bp deletion with sgRNA_K01 was successful but it did not change the coding sequence.

(B) Relative expression level of Mp*DELLA* determined by RT-qPCR in 14-day-old gemmalings.

(C) Relative expression level of Mp*PIF* determined by RT-qPCR in 14-day-old gemmalings of $_{pro}$*35S:Cit*-Mp*PIF* Mp*DELLA-GR* lines.

(D) Microscopic image of the apical notch of *g*Mp*DELLA-Cit* gemma showing MpDELLA-Cit nuclear localization. Scale bar, 200 μm.

(E) Morphology of Mp*DELLA-GR* plants, grown from gemmae for 14 days with mock or different concentrations of DEX. Scale bar, 5 mm.

(F) Measurement of plant sizes in Mp*DELLA-GR* gemmalings, grown from gemmae with mock or 1 μM DEX for 14 days. n=27.

(G) Apical notches of 7-day-old Mp*DELLA-GR* gemmalings, treated with mock or 1 μM DEX for two days and labelled with EdU (yellow signals). Plant boundaries are marked with white lines, and blue color indicates the area occupied by dividing cells. Scale bar, 500 μm.

(H) Number of EdU-labelled nuclei in the apical notches of 7-day-old Mp*DELLA-GR* gemmalings, treated with mock or 1 μM DEX for two days. n=12.

(I) Quantification of actively dividing area in the apical notches of 7-day-old Mp*DELLA-GR* gemmalings, treated with mock or 1 μM DEX for two days. n=12.

(J) GUS-stained thallus of 21-day-old Mp*DELLA* reporter lines, showing the range of promoter activity across the thallus ($_{pro}$Mp*DELLA:GUS*, Scale bar, 5 mm) or MpDELLA protein accumulation in developing (black arrow) and mature (white arrow) gemma cups (agar sectionings of *g*Mp*DELLA-GUS*. Scale bars, 200 μm).

(K) Genotype information for the Mp*smr*^{ge} Mp*DELLA-GR* lines. Predicted protein products from wild-type and genome-edited Mp*SMR* locus were illustrated (purple boxes: CDKI functional domains; dark-grey shade: frameshifts caused by genome editing). Sequences of wild-type and both CRISPR/Cas9-derived alleles were shown in alignments. In A, B, error bars represent SE (n=3). In E, F, G, dots represent individual plants and horizontal lines represent mean values. Statistical groups were determined by Tukey's Post-Hoc test ($p<0.05$) after one-way ANOVA.

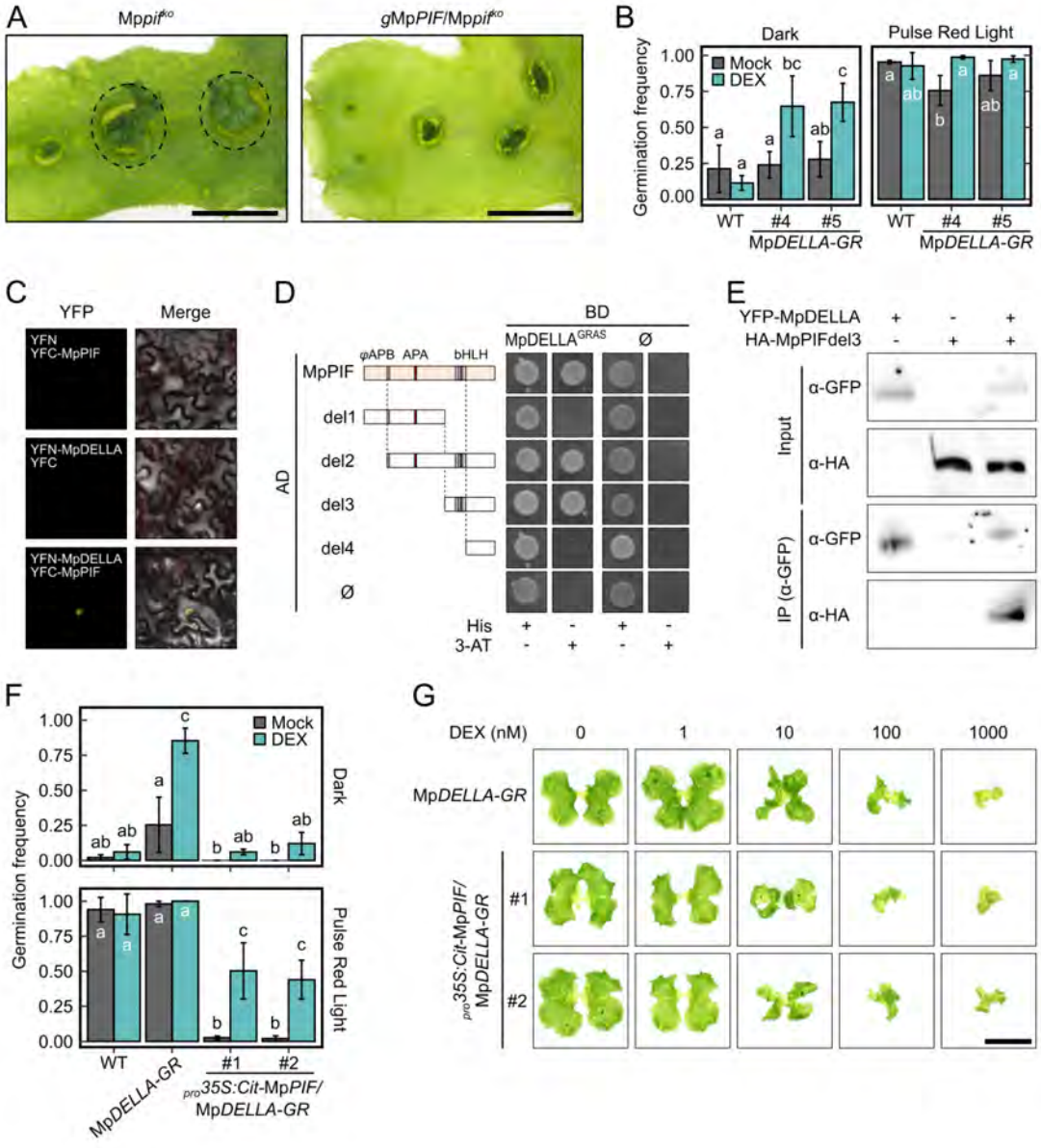
A
Mppif^ko
gMpPIF/Mppif^ko
B
Dark
Pulse Red Light
Mock
DEX
Germination frequency
WT
#4
#5
MpDELLA-GR
C
YFP
Merge
YFN
YFC-MpPIF
YFN-MpDELLA
YFC
YFN-MpDELLA
YFC-MpPIF
D
BD
MpDELLA^GRAS
Ø
φAPB
APA
bHLH
MpPIF
del1
del2
del3
del4
AD
His
3-AT
E
YFP-MpDELLA
HA-MpPIFdel3
Input
IP (α-GFP)
α-GFP
α-HA
F
Mock
DEX
Dark
Pulse Red Light
Germination frequency
WT
MpDELLA-GR
pro35S:Cit-MpPIF/
MpDELLA-GR
#1
#2
G
DEX (nM)
0
1
10
100
1000
MpDELLA-GR
pro35S:Cit-MpPIF/
MpDELLA-GR

Figure S2. Physical and functional interaction between MpDELLA and MpPIF. Related to Figure 2.

(A) Images of 28-day-old plants showing premature gemmae germination inside the cups of Mp*pif*^{ko} and the complemented line (*g*Mp*PIF*/Mp*pif*^{ko}). Dashed circles indicate non-dormant gemma cups. Scale bar, 5 mm.

(B) Germination frequencies of the wild-type and Mp*DELLA-GR* gemmae under different light conditions. Gemmae were imbibed and treated without (Dark) or with a pulse of red light (4500 µmol photons m^{-2}) followed by incubation in the dark. Dark grey and turquoise columns represent gemmae supplemented with mock or 1 µM DEX, respectively.

(C) Bimolecular fluorescence complementation assays showing MpDELLA-MpPIF interaction in *N. benthamiana* abaxial leaves.

(D) Physical interaction between MpDELLA GRAS domain and MpPIF bHLH domain shown by yeast two-hybrid assays of MpPIF deletion fragments. Although there is no conserved APB domain in MpPIF, its theoretical position was marked by *ψ*APB and used for fragmentation. MpPIF amino acids present on each fragment are 1-472 (del1), 132-760 (del2), 473-760 (del3) and 588-760 (del4). Histidine (His) supplemented media used as growth control. 5 mM 3-amino-1,2,4-triazole (3-AT) was added to His-depleted medium.

(E) Physical interaction between YFP-MpDELLA and HA-MpPIFdel3 (aa 473-760) shown by co-immunoprecipitation after agroinfiltration in *N. benthamiana* leaves.

(F) Germination frequencies of Mp*DELLA-GR* gemmae with additional expression of Mp*PIF* ($_{pro}$*35S:Cit*-Mp*PIF*) under different light conditions as indicated in (B). Dark grey and blue columns represent gemmae supplemented with mock or with 1 µM DEX, respectively.

(G) Morphology of 14-day-old Mp*DELLA-GR* and $_{pro}$*35S:Cit*-Mp*PIF*/Mp*DELLA-GR* plants, grown with different concentrations of DEX. Scale bar, 1 cm.

In B, F, error bars represent standard deviation from three independent experiments (n = 50 per experiment). Statistical groups were determined by Tukey's Post-Hoc test ($p<0.05$) following ANOVA analysis.

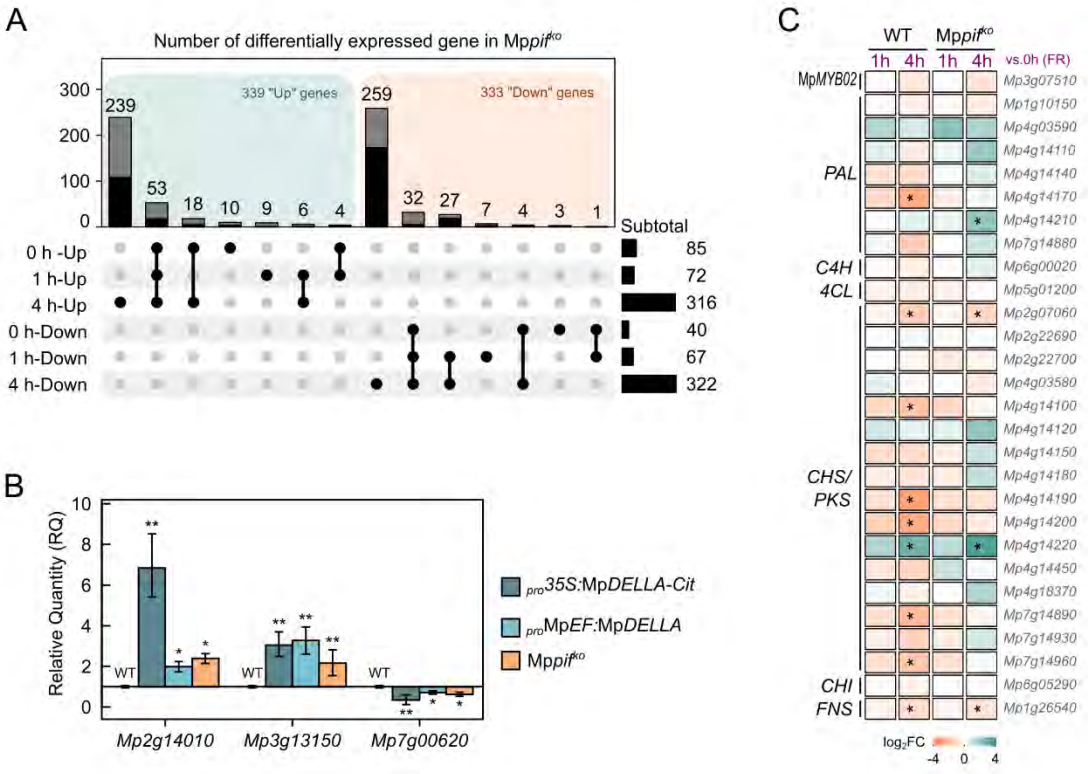

Figure S3. Mp*PIF*-dependent gene expression changes in response to far-red light. Related to Figure 3.

(A) UpSet plot showing differentially expressed genes between Mp*pif*^{ko} and the wild-type at different time points after far-red light (FR) irradiation. Black proportions in the top column plot represent genes ever changed significantly (with |log2FC|>1 and adjusted p<0.01 calculated by DESeq2) in response to far-red treatment in either genotypes.

(B) Relative expression level of selected genes by RT-qPCR, as a verification for the RNA-seqs. Error bars represent standard deviation from three biological replicates. Asterisks indicate statistically significant differences with respect to the wild type (*, p<0.05; **, p<0.01, after a Student's t-test)

(C) Fold changes in expression (log2 scale) of genes related to flavonoid biosynthesis, compared to time point 0 in both genotypes. Asterisks indicate genes considered as significantly changed (with |log2FC|>1 and adjusted p<0.01 calculated by DESeq2).

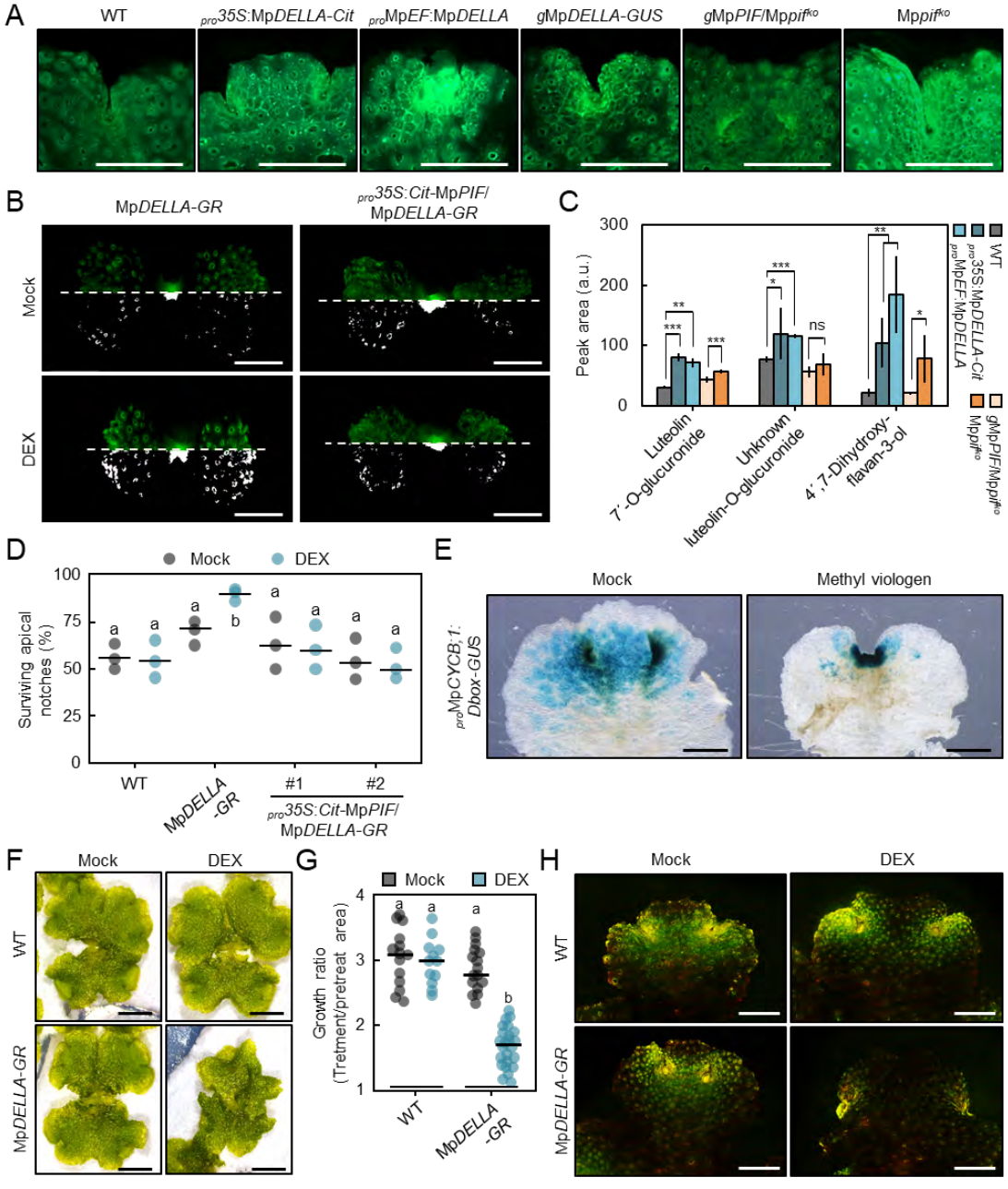
A
WT
proMpEF:MpDELLA
gMpDELLA-GUS
gMpPIF/Mppifko
Mppifko
B
MpDELLA-GR
pro35S:Cit-MpPIF/
MpDELLA-GR
Mock
DEX
C
Peak area (a.u.)
300
200
100
0
Luteolin
7´-O-glucuronide
Unknown
luteolin-O-glucuronide
4´,7-Dihydroxy-
flavan-3-ol
WT
pro35S:MpDELLA-Cit
proMpEF:MpDELLA
gMpPIF/Mppifko
Mppifko
D
Mock
DEX
Surviving apical
notches (%)
100
75
50
25
0
WT
MpDELLA
-GR
#1
#2
pro35S:Cit-MpPIF/
MpDELLA-GR
E
Mock
Methyl viologen
proMpCYCB;1:
Dbox-GUS
F
Mock
DEX
WT
MpDELLA-GR
G
Mock
DEX
Growth ratio
(Tretment/pretreat area)
4
3
2
1
WT
MpDELLA
-GR
H
Mock
DEX
WT
MpDELLA-GR

Figure S4. Involvement of MpDELLA in the response to oxidative stress. Related to Figure 4.

(A) Images of apical region of Figure 4A gemmalings, stained by DPBA. More intense fluorescent signals denote higher general flavonoid content. Scale bar, 1 mm.

(B) Images showing DPBA staining of 9-day-old Mp*DELLA-GR* and $_{pro}$*35S:Cit*-Mp*PIF* Mp*DELLA-GR* gemmalings, grown with or without 1 µM DEX for 3 days. Upper halves, original picture taken with GFP filter; Lower halves, pseudo-color intensity binary maps (threshold at 30%) to facilitate the comparison of the differences in fluorescence signal between images. Scale bar, 2 mm.

(C) Differentially accumulated flavonoid-related compounds in different genotypes as found by untargeted metabolomics analyses. Original data with individually detected ions and parameters of detection can be found in Table S1.

(D) Percentage of surviving apical notches after a 10-day treatment with 100 µM methylviologen (MV). Mp*DELLA-GR* induction with 1 µM DEX started one day earlier before MV application and was further maintained throughout the stress treatment.

(E) Images of 13-day-old Mp*CYCB;1-GUS* Mp*DELLA-GR* plants stained for GUS activity after mock or 10 µM MV treatment for 6 days. Scale bar, 1 mm.

(F) Morphology of 14 days-old wild-type and Mp*DELLA-GR* plants grown for three days after local application of 20 µM DEX at the apical notch. Scale bar, 4 mm.

(G) Quantification of the growth ratio in F, accounted as the thallus projection area three days after DEX treatment versus thallus projection area the day of application.

(H) Images of DBPA staining showing the effect of apical notch local DEX application in plants identical to those in F. Scale bar, 2 mm.

In C, fold changes and p-values from Student's t-tests are calculated with quantifications from four samples per genotype with the sole exception of Tak-1 (three samples). In D, E dots represent biological replicates and horizontal lines median values from three independent experiments, in G, dots represent individual measurements in two independent experiments, statistical support is provided by one-way ANOVA analysis, and groups determined by Tukey's Post-Hoc test ($p<0.01$).

ESI	Compound	Mass	Rt [s]	Ion annotation	Tak-1[a]			$_{pro}$35S:Mp*DELLA-Cit*				$_{pro}$Mp*EF1*:Mp*DELLA*			
					1	2	3	1	2	3	4	1	2	3	4
Positive	Putative 4-methylumbelliferone	177.0567	544.87	[M+H]+	21.091	9.238	6.973	35.753	31.979	26.927	33.904	19.002	34.181	9.378	32.949
		149.0237	544.97	[M+H-C2H4]+	120.450	51.369	39.169	220.470	201.774	150.897	217.772	110.277	210.782	52.009	206.282
	Unknown luteolin-O-glucuronide	463.0881	321.49	[M+H]+	70.867	81.062	76.861	83.134	85.018	138.076	170.261	120.674	113.016	114.514	112.523
		287.0552	322.17	[M+H-C6H8O6]+	8.330	9.726	8.906	10.125	9.715	17.109	9.636	14.085	13.621	13.295	13.124
	Luteolin 7´-O-glucuronide	463.0879	304.55	[M+H]+	33.427	30.285	27.656	79.369	85.051	72.045	85.394	64.441	81.315	66.450	73.482
		287.0552	305.12	[M+H-C6H8O6]+	3.248	3.025	2.674	7.240	7.497	7.124	7.093	5.411	7.483	4.751	6.807
	Caffeoylputrescine	251.1394	244.74	[M+H]+	21.915	20.272	20.598	43.297	40.557	52.869	44.964	35.856	47.033	36.970	44.718
		234.1123	244.74	[M-NH3]+	5.959	5.671	5.694	12.087	11.322	14.323	12.352	9.746	13.187	10.249	12.610
		205.1317	244.79	[M+H-C2H4]+	1.430	1.320	1.347	3.024	2.706	3.192	3.037	2.415	3.179	2.394	3.014
		122.0949	244.68		5.842	5.588	5.638	11.766	11.031	14.303	12.336	9.887	13.037	10.167	12.394
		105.0687	244.74	[M-caffeoyl]+	1.064	1.041	1.101	2.191	2.087	2.651	2.276	1.839	2.434	1.903	2.332
	4´,7-Dihydroxyflavan-3-ol	241.0868	467.67	[M+H-H2O]+	28.571	18.823	16.590	87.209	114.125	255.724	59.885	268.571	131.078	198.868	138.874
		147.0449	467.78	[M+H-H2O]+	17.491	11.582	10.106	50.208	67.694	150.714	34.332	151.692	74.621	117.947	81.725
Negative	Luteolin 7´,3´-O-diglucuronide	637.1044	291.69	[M-H]-	113.605	75.138	66.165	273.490	356.434	297.449	270.798	101.822	99.414	91.258	115.389
	Unknown luteolin-O-glucuronide	461.0724	324.14	[M-H]-	60.278	70.459	65.381	81.516	72.894	115.511	74.171	95.952	96.811	89.242	91.702
		285.0396	324.60	[M-H-C6H8O6]-	7.518	7.998	7.398	9.322	8.309	13.589	8.502	10.792	11.105	10.173	11.279
	Luteolin 7´-O-glucuronide	461.0723	307.70	[M-H]-	23.615	19.309	16.734	53.019	67.125	57.540	63.409	34.938	58.281	54.890	59.098
	Caffeoylputrescine	249.1232	248.15	[M-H]-	6.795	7.014	7.287	11.676	13.234	19.408	15.030	10.248	15.045	10.600	14.798
		127.0477	248.35		0.193	0.088	0.184	0.293	0.331	0.302	0.370	0.270	0.380	0.291	0.351
	putative octopamine hexose	314.1211	136.78	[M-H]-	0.798	0.785	0.514	8.660	9.518	1.918	15.348	3.195	6.541	2.765	5.865

ESI	Compound	Mass	Rt [s]	Ion annotation	*g*Mp*PIF*/Mp*pif*^{ko} 1	2	3	4	Mp*pif*^{ko} 1	2	3	4
Positive	**Putative 4-methylumbelliferone**	177.0567	544.87	[M+H]+	10.859	12.647	17.819	11.201	11.894	11.520	20.594	28.370
		149.0237	544.97	[M+H-C2H4]+	64.320	71.843	102.214	63.689	67.850	64.421	129.803	192.782
	Unknown luteolin-O-glucuronide	463.0881	321.49	[M+H]+	41.856	60.676	63.472	58.140	64.634	62.774	95.748	53.347
		287.0552	322.17	[M+H-C6H8O6]+	5.052	7.491	7.897	7.264	8.295	8.188	11.890	6.524
	Luteolin 7´-O-glucuronide	463.0879	304.55	[M+H]+	37.325	45.574	42.137	49.499	56.992	53.588	61.097	55.189
		287.0552	305.12	[M+H-C6H8O6]+	3.584	3.825	4.896	4.345	5.195	4.542	5.363	3.975
	Caffeoylputrescine	251.1394	244.74	[M+H]+	17.119	21.090	22.467	19.943	28.859	26.182	43.316	31.139
		234.1123	244.74	[M-NH3]+	4.658	5.820	5.996	5.547	7.961	7.387	11.901	8.834
		205.1317	244.79	[M+H-C2H4]+	1.132	1.445	1.419	1.298	1.932	1.746	2.934	2.279
		122.0949	244.68		4.577	5.827	5.987	5.426	7.883	7.236	11.716	8.591
		105.0687	244.74	[M-caffeoyl]+	0.849	1.109	1.191	1.040	1.532	1.399	2.242	1.663
	4´,7-Dihydroxyflavan-3-ol	241.0868	467.67	[M+H-H2O]+	22.074	17.469	41.774	22.896	128.454	91.125	46.065	46.374
		147.0449	467.78	[M+H-H2O]+	13.217	10.569	25.255	14.127	74.677	51.880	26.410	26.581
Negative	**Luteolin 7´,3´-O-diglucuronide**	637.1044	291.69	[M-H]-	67.493	96.628	122.130	104.665	111.467	102.963	148.882	47.878
	Unknown luteolin-O-glucuronide	461.0724	324.14	[M-H]-	38.255	50.248	55.562	51.614	52.933	52.704	78.400	42.887
		285.0396	324.60	[M-H-C6H8O6]-	4.614	6.043	6.496	6.293	6.824	6.302	9.680	5.444
	Luteolin 7´-O-glucuronide	461.0723	307.70	[M-H]-	26.720	32.180	30.252	38.669	39.615	36.638	45.397	42.585
	Caffeoylputrescine	249.1232	248.15	[M-H]-	5.263	6.190	7.376	6.741	8.097	7.471	14.310	9.555
		127.0477	248.35		0.133	0.119	0.166	0.101	0.201	0.200	0.339	0.241
	putative octopamine hexose	314.1211	136.78	[M-H]-	2.782	1.292	3.151	2.581	8.146	6.462	3.606	8.787

Table S1. Differentially accumulated flavonoid-related metabolites in different lines, related to Figure S4C

[a]Tak-1_4 was discarded due to deviation.
Dark grey-shaded cells were discarded from posterior analysis due to deviation.

Name	Sequence (5' to 3')	Used for
MpDELLA_Fw2	GGGGACAAGTTTGTACAAAAAAGCAGGCT TAATGGATTCCTCTGCCGATTACG	pENTR221-MpDELLA
MpM5DELLA_Fw2	GGGGACAAGTTTGTACAAAAAAGCAGGCT ACATCTCGGATTCAATGGCTGGAG	pENTR221-MpDELLA^{GRAS}
pMpDELLA_Fw2	GGGGACAAGTTTGTACAAAAAAGCAGGCT CGGCGTAGGAGATGGGCACTTG	pENTR221-$_{pro}$MpDELLA, pENTR221-gMpDELLA
pMpDELLA_Rv2	GGGGACCACTTTGTACAAGAAAGCTGGGT AACAGCAGGCAATTATCACTCTTCG	pENTR221-$_{pro}$MpDELLA
MpDELLA_Rv2	GGGGACCACTTTGTACAAGAAAGCTGGGT AGGAACAATGCCATGCCGATG	pENTR221-MpDELLA, pENTR221-MpDELLA^{GRAS}, pENTR221-gMpDELLA
CACC-MpDELLA-CDS-F	CACCATGGATTCCTCTGCCG	pENTR-MpDELLA
MpDELLA-CDS-ns-R	GGAACAATGCCATGCCGATG	pENTR-MpDELLA
SalI-MpDELLApro-F	CGCGTCGACATAGAATACGCAACTTTATGGCA	pENTR1A-$_{pro}$MpDELLA-short
NotI-MpDELLApro-R	AAAGCGGCCGCTAACAGCAGGCAATTATCACT CT	pENTR1A-$_{pro}$MpDELLA-short
MpDELLApro1-IF-F	AGGAACCAATTCAGTCGACACGGCGTAGGAGA TGGG	pENTR1A-$_{pro}$MpDELLA, pENTR1A-gMpDELLA
MpDELLApro2-IF-R	CCTTTTGCCATAAAGTTGCGTATT	pENTR1A-$_{pro}$MpDELLA, pENTR1A-gMpDELLA
MpDELLA-cassette-IF-F	AATTGCCTGCTGTTA ATGGATTCCTCTGCCGATTACG	pENTR1A-gMpDELLA-short
MpDELLA-cassette-IF-R1	ATATCTCGAGTGCGG GGAACAATGCCATGCCGATG	pENTR1A-gMpDELLA-short
SalI-MpCYCB-5´ [a]	GTCGACTCAAAAATTCTCCTCCGTACA	pENTR1A-MpCYCB;1-Dbox
MpCYCB-116-3´-pENTR	GCCCCGAAGCAGGAGCAATGT	pENTR1A-MpCYCB;1-Dbox
MpPIF_1F	CACCATGAGTCACCTCGTTC	pENTR-MpPIF-Stop
MpPIF_0R	AAGCAAGCGTGGAAATCAAG	pENTR-MpPIF-Stop
MpPIF_Fw	ATGAGTCACCTCGTTCCCG	pCR8-MpPIF pCR8-MpPIFdel1
MpPIF_Rv	TTGGGGGGCTCCACCGCCC	pCR8-MpPIF pCR8-MpPIFdel2-4
MpPIFdel1_Rv	GGCCTCTTTCCCTCTATC	pCR8-MpPIFdel1
MpPIFdel2_Fw	CAGGAAGACGAGATGGTG	pCR8-MpPIFdel2
MpPIFdel3_Fw	GCATCTAGTGGCAAGAGA	pCR8-MpPIFdel3
MpPIFdel4_Fw	CAGATGATGTCCATGAGA	pCR8-MpPIFdel4
sgDELLA_V01_F	CTCGCACGGTTCTGGGTGTTTCTC	pMpGE_En03-MpDELLA-sgV01
sgDELLA_V01_R	AAACGAGAAACACCCAGAACCGTG	pMpGE_En03-MpDELLA-sgV01
sgDELLA_V02_F	CTCGTACAATCCCGCAGATCTGGC	pMpGE_En03-MpDELLA-sgV02
sgDELLA_V02_R	AAACGCCAGATCTGCGGGATTGTA	pMpGE_En03-MpDELLA-sgV02
sgDELLA_V03_F	CTCGCATGCCGGACATGTACCCAG	pMpGE_En03-MpDELLA-sgV03
sgDELLA_V03_R	AAACCTGGGTACATGTCCGGCATG	pMpGE_En03-MpDELLA-sgV03
sgDELLA_K01_F	CTCGCGCAAAGTAGGAAGACGC	pMpGE_En03-MpDELLA-sgK01
sgDELLA_K01_R	AAACGCGTCTTCCTACTTTGCG	pMpGE_En03-MpDELLA-sgK01
sgDELLA_K02_F	CTCGGAGGAATCCATTAACAGC	pMpGE_En03-MpDELLA-sgK02
sgDELLA_K02_R	AAACGCTGTTAATGGATTCCTC	pMpGE_En03-MpDELLA-sgK02
sgDELLA_K03_F	CTCGGTGTGAGCCAGGAGCTGC	pMpGE_En03-MpDELLA-sgK03
sgDELLA_K03_R	AAACGCAGCTCCTGGCTCACAC	pMpGE_En03-MpDELLA-sgK03
sgDELLA_K04_F	CTCGTTCGTCGAAGCTCTGGCC	pMpGE_En03-MpDELLA-sgK04
sgDELLA_K04_R	AAACGGCCAGAGCTTCGACGAA	pMpGE_En03-MpDELLA-sgK04
genoMpDELLA_Kyoto-F	TGTCCCAATCCTTCCTTCGC	MpDELLA genotyping
genoMpDELLA_Kyoto-R	GGACACGAACGATGAATGCG	MpDELLA genotyping
sgRNA_MpSMR_F	CTCGGTCGGAGGACATGAGTCAAC	pEn03-MpSMR-sgRNA
sgRNA_MpSMR_R	AAACGTTGACTCATGTCCTCCGAC	pEn03-MpSMR-sgRNA
genoMpSMR_F	GGTAGTTCCTCTGGCTCAAG	MpSMR genotyping
genoMpSMR_R	CTGTGATACGGTAGGAATGAGT	MpSMR genotyping

MpEF1−qPCR_F	AAGCCGTCGAAAAGAAGGAG	qPCR (Mp3g23400)
MpEF1−qPCR_R	TTCAGGATCGTCCGTTATCC	qPCR (Mp3g23400)
MpDELLA-RT-F1	AGTTCTACGAGACTTGTC	qPCR (Mp5g20660)
MpDELLA-RT-R1	ATGTATCCGCTTGTGATT	qPCR (Mp5g20660)
MpPIF-qPCR-F1	CAGCCGATGAGTATGGATGC	qPCR (Mp3g17350)
MpPIF-qPCR-R1	AGATGATGGAGCGAATGCTG	qPCR (Mp3g17350)
MpPALd-qPCR-F	CTGCTAAGAAATCTCTATTCAC	qPCR (Mp7g14880)
MpPALd-qPCR-R	ACTAGTGGCATCATCTATGTAA	qPCR (Mp7g14880)
MpPALb-qPCR-F	CACTTACGGTGTCACTACAG	qPCR (Mp4g14110)
MpPALb-qPCR-R	ATCAACTCTCTCTGTAAGTCG	qPCR (Mp4g14110)
MpC4Ha-qPCR-F	GAGAAAGCAGCTATTGATTAC	qPCR (Mp8g00020)
MpC4Ha-qPCR-R	GTAGTCTCAATAGCAGCAAC	qPCR (Mp8g00020)
MpCHS/STBS-qPCR-F	AGTTCGCTCGAATTTGTAAG	qPCR (Mp4g18370)
MpCHS/STBS-qPCR-R	AAGTGAGGGATCCTTGTAC	qPCR (Mp4g18370)
MpGH3B-qPCR-F	GTAAACTGAAAATGCTACCTGT	qPCR (Mp2g14010)
MpGH3B-qPCR-R	GTTGATTTCATGTGAAACC	qPCR (Mp2g14010)
MpKSb-qPCR-F	GACCTTCCGTACAATCTC	qPCR (Mp3g13150)
MpKSb-qPCR-R	GATGAAGGGGTATTTTGC	qPCR (Mp3g13150)
MpFUT-qPCR-F	TGACTTCACATATGGTTATACC	qPCR (Mp7g00620)
MpFUT-qPCR-R	CATAATCGTATAAGCTCTTGAC	qPCR (Mp7g00620)

Table S2. List of oligonucleotides, related to STAR methods.

[a]The last nucleotide of this primer does not match with the current reference genome, though the amplification was successful and confirmed by sequencing.

Additional overhangs for proper cloning (Gateway/restriction site/sticky end) are marked in red; start codons are underlined.

Supplemental Dataset 1

Click here to access/download

Supplemental Videos and Spreadsheets

Hernandez-Sun-DataS1.xlsx